Sumoylation of the human histone H4 tail inhibits p300-mediated transcription by RNA polymerase II in cellular extracts

Calvin J. A. Leonen,[*] Miho Shimada,[**‡] Caroline E. Weller,[*] Tomoyoshi Nakadai,[**†] Peter Hsu,[#¶] Patrick M. M. Shelton,[*] Martin Sadilek,[*] Ning Zheng,[#] Robert G. Roeder,[**] Champak Chatterjee[*]

* Department of Chemistry, University of Washington, Seattle, WA 98195.

** Laboratory of Biochemistry and Molecular Biology, The Rockefeller University, New York, NY, USA.

[#] Department of Pharmacology, University of Washington, Seattle, WA, 98195; Howard Hughes Medical Institute, University of Washington, Seattle, WA 98195.

[‡] Present address: Department of Molecular Biology, Yokohama City University, Kanagawa 2360004, Japan

[†] Present address: Project for Cancer Epigenomics, Cancer Institute of JFCR, Tokyo, Japan, 135-8550.

[¶] Present address: Department of Structural Biology, Genentech, 1 DNA Way, South San Francisco, CA 94080.

Email to: chatterjee@chem.washington.edu and roeder@rockefeller.edu

Abstract

Post-translational modification of histone H4 by the small ubiquitin-like modifier (SUMO) protein was associated with gene repression. However, this could not be proven due to the challenge of site-specifically sumoylating H4 in cells. Biochemical crosstalk between SUMO and other histone modifications, such as H4 acetylation and H3 methylation, that are associated with active genes also remains unclear. We addressed these challenges in mechanistic studies using H4 chemically modified at Lys12 by SUMO-3 (H4K12su) that was incorporated into mononucleosomes and chromatinized plasmids. Mononucleosome-based assays revealed that H4K12su inhibits transcription-activating H4 tail acetylation by the histone acetyltransferase p300, and transcription-associated H3K4 methylation by the extended catalytic module of the Set1/COMPASS histone methyltransferase complex. Activator- and p300-dependent in vitro transcription assays with chromatinized plasmids revealed H4K12su inhibits RNA polymerase II-mediated transcription and H4 tail acetylation. Thus, we have uncovered negative biochemical crosstalk with acetylation/methylation and the direct inhibition of RNAPII-mediated transcription by H4K12su.

Introduction

Chromatin is Nature's elegant architectural solution to the challenge of packing approximately 3 billion base-pairs of human genomic DNA in an average nuclear volume of only about 500 cubic microns. Histones constitute the main protein component of chromatin and their reversible post-translational modifications (PTMs), or *marks*, regulate chromatin structure and function by a range of direct and indirect mechanisms.[1] Based upon their association with either transcriptionally active or silenced regions of chromatin, histone marks were proposed to constitute an epigenetic *code* for gene function.[2] As a consequence of their early discovery and the development of modification-specific chemical and molecular biological tools, marks such as methylation,[3] acetylation[4] and ubiquitylation[5] have been extensively investigated in vitro and in cell culture. In contrast, histone modification by the small ubiquitin-like modifier (SUMO) protein is a poorly understood mark due both to its very low abundance in cells, which prevents the isolation of sumoylated histones in quantities required for biochemical analysis, and to a lack of sumoylated histone-specific antibodies for cellular studies. First reported in human HEK293T and P493-6 B cells by Shiio and Eisenman,[6] histone sumoylation also occurs in yeast,[7] parasitic protozoans,[8] and plants.[9] Similar to histone ubiquitylation, sumoylation occurs on all core histones, the linker histone H1, the histone variants H2A.Z and H2A.X and the centromeric histone variant Cse4 in yeast.[10, 11] Pioneering efforts to identify specific lysine sites of sumoylation identified K12 in histone H4 as a major recurring site of sumoylation by SUMO-2/3 (H4K12su),[12, 13] although multiple proximal lysines in the H4 N-terminal tail may also be enzymatically sumoylated in vitro.[10] Genetic studies in yeast and human cells have typically associated H4 sumoylation with the repression of gene transcription, although mechanistic studies of the direct roles for histone

sumoylation in human cells have remained intractable due to the dynamic nature and low abundance of sumoylation.[6, 14]

In an effort to understand the direct effects of H4K12su in chromatin, we previously applied a disulfide-directed chemical sumoylation strategy to generate uniformly and site-specifically sumoylated nucleosome arrays.[15] Biophysical studies of chromatin-array compaction remarkably showed that H4K12su is incompatible with the compact chromatin structures seen in transcriptionally silent heterochromatin. Subsequent biochemical studies revealed that H4K12su stimulates intranucleosomal activity of the H3K4me2-specific histone demethylase LSD1.[16] These studies suggested that sumoylated H4 does not directly enable heterochromatin formation and may instead act by recruiting LSD1 to genes. However, a potentially direct effect of histone H4 sumoylation on promoter-driven transcription by RNA polymerase II (RNAPII) and associated initiation factors that are key for efficient eukaryotic gene transcription has remained unknown.

Pioneering studies of the reconstitution of class II promoter-driven accurate eukaryotic transcription in both nuclear extracts and purified systems has led to insights into roles for histone modifications in gene function.[17, 18] The ability to reconstitute chromatinized plasmid templates using chemically modified histones enables studies of the roles of specific histone modifications in transcription and investigations of their crosstalk with key enzymes associated with transcription initiation and elongation.[19] Multiple proteins involved in gene transcription bind to and modify histone tails, which enables the remodeling of chromatin prior to and during transcription. One such modification, acetylation of lysine side-chains on H3 and H4 by the acetyltransferase p300, is necessary for efficient activator-driven transcription of both 11-nm chromatin[20] and 30-nm linker histone H1-containing heterochromatin, likely through mechanisms that include direct

decompaction of chromatin upon H4K16 acetylation and octamer eviction by the chromatin remodeler NAP1.[21, 22]

Due to their proposed opposing roles in gene transcription, we investigated the precise nature of biochemical crosstalk between histone sumoylation and histone acetylation by p300. Histone H4 site-specifically sumoylated at Lys12 (H4K12su) was synthesized with the aid of a traceless ligation auxiliary, 2-aminooxyethanethiol,[23] and then incorporated into histone octamers for subsequent reconstitution of cognate mononucleosomes and chromatinized plasmids. Each sumoylated substrate was subjected to acetyltransferase assays with the full-length p300 enzyme, which revealed a consistent inhibition of acetylation in the H4K12su tail. Consistent with this observation and requirements for both H3 and H4 acetylation for in vitro transcription of chromatin,[20] replacing wild-type (wt) H4 with H4K12su in chromatinized plasmid templates dramatically inhibited p300-dependent, RNAPII-mediated transcription in vitro. Bottom-up mass spectrometry on chromatinized histones, following a novel in-gel desumoylation protocol, revealed decreased acetylation in H4K12su by p300 when compared to wt H4. Consistent with a role in gene repression, H4K12su also inhibited H3K4 methylation by the extended catalytic module of the Set1/COMPASS methyltransferase complex.[24] Collectively, our observations provide the first unambiguous biochemical demonstration that sumoylated histone H4 directly inhibits RNAPII-mediated transcription from chromatin templates, and reveal its direct negative crosstalk with histone acetylation by p300 and methylation by Set1/COMPASS that are strongly associated with active gene transcription.

Results

Reconstitution of site-specifically sumoylated octamers and nucleosomes. Site-specifically sumoylated human histone H4 at Lys12, H4K12su, was obtained by a semisynthetic strategy using

the ligation auxiliary 2-aminooxyethanethiol (Figure 1A and 1B).[16] The semisynthetic sumoylated H4 was incorporated into octamers with purified recombinant human histones H2A, H2B and H3 (Figure 1C). Nucleosomes were reconstituted from sumoylated octamers using the 147 bp Widom 601 double-stranded DNA (Figure 1D).

Histone octamer acetylation by p300. We previously showed that H4K12su stimulates activity of the H3K4me1/2 demethylase, LSD1, in the context of a LSD1-CoREST sub-complex.[16] The stimulation of histone deacetylase (HDAC) activity of the Set3c complex in yeast was also recently proposed for sumoylated histone H2B.[25] Although the erasure of specific methyl and acetyl marks in the H3 and H4 tails may facilitate the transcriptionally repressed state of chromatin, there remains no information regarding the re-installation of these marks by the corresponding writer enzymes in the presence of H4K12su. Key among the histone acetyltransferases is the enzyme p300 that is recruited to chromatin by transcriptional activators for histone tail acetylation prior to transcription initiation.[20, 26, 27] Given its essential role in transcription, we investigated the effect of H4K12su on histone acetylation by p300 prior to and during transcription by RNAPII.

To investigate the direct biochemical crosstalk between H4K12su and acetylation, a Western-blot-based histone acetyltransferase (HAT) assay was developed using a sequence-independent pan-acetyllysine antibody to detect lysine acetylation in all four histones (Figure S1A). In order to effectively compare acetylation of wt H4 with H4K12su and to strictly exclude any acetylation of the surface-exposed lysines in SUMO-3 attached to H4 (Figure S1B), it was proteolyzed from H4K12su prior to analysis. To this end, after acetylation by p300, the assay product was heat inactivated at 65 ^{o}C for 10 min, followed by addition of the purified catalytic domain of human SENP2 containing residues 365-590 (Figure S1C).[28] Heat inactivation precluded

p300 activity during desumoylation, and enabled the direct comparison of acetylation status in H4 and H4K12su.

Histone octamers containing wt H4 were first acetylated with full-length p300 immuno-affinity purified from HEK293T cells with an N-terminal FLAG epitope-tag (Figure S1D).[29] Western blot analysis showed the robust acetylation of all four histones (Figure 1E top panel and S1E). This is consistent with previous in vitro assays that revealed acetylation of all four histones by p300.[30] Strikingly, H4 from octamers containing H4K12su was devoid of acetylation, including H4K16ac (Figure 1E bottom panel), which is strongly associated with chromatin decompaction and active gene transcription.[21, 31, 32] Importantly, the inhibition of H4 tail acetylation does not arise from allosteric inactivation of p300, based on the observation that the other histones in H4K12su octamers were acetylated to the same extent as in wt H4 octamers. Additionally, Western blots confirmed that SUMO-3 did not inhibit p300 autoacetylation, which is associated with robust acetyltransferase activity (Figure S1F). Hence the inhibition of H4 acetylation in H4K12su is likely due to lysine acetylation site-occlusion by proximal SUMO-3 in the H4 tail.

Mononucleosome acetylation by p300. The histone acetylation assay was next undertaken with mononucleosomes containing either wt H4 or H4K12su. We failed to see significant nucleosome acetylation with pan-acetyllysine antibodies with or without pre-incubation of p300 with acetyl-CoA prior to the addition of nucleosomes (Figure S1G). Due to the significantly decreased activity of p300 with nucleosomal substrates, a [^{3}H]-acetyl-CoA co-factor was employed and the transfer of acetyl groups to histones observed by fluorography. H4 acetylation was also suppressed in mononucleosomes containing H4K12su, but not in unmodified H4 mononucleosomes (Figure 1F). Our results unequivocally suggested that SUMO-3 in the H4 tail is inhibitory toward p300-mediated acetylation of chromatin, a process that is necessary for active gene transcription.

Based on the lower acetyltransferase activity observed with mononucleosomes than with octamers, we wondered if dsDNA may inhibit p300 activity. To test this, an equimolar amount of free 147 bp Widom 601 dsDNA was included in the octamer acetylation assay. The presence of DNA was sufficient to inhibit p300 activity to a similar extent as observed with mononucleosomes (Figure S1H). This unexpected inhibition of p300 activity by free DNA suggests that additional factors, such as transcription factor and RNAPII binding, enable robust p300 activity on histones during transcription initiation and elongation.

The effect of H4K12su on cell-free transcription from chromatinized templates. Based on our observation that H4K12su inhibits the acetylation of key H4 tail residues that are associated with p300-dependent active transcription, including H4K16 that is acetylated in euchromatin, we sought to investigate the direct effect of H4K12su on transcription in our reconstituted cell-free system. These assays employed a p300/Gal4-VP16-dependent transcription system using chromatinized plasmids assembled with reconstituted octamers containing either wt H4 or H4K12su (Figure 2A). The plasmid DNA template consisted of five *gal4* binding sites and a ~400 bp G-less cassette.[27] Due to the absence of any engineered strong nucleosome positioning sequences in the template, chromatinization was undertaken with the histone chaperone NAP1 and the chromatin remodelers Acf1 and ISWI (Figure S2). Limited micrococcal nuclease digestion of the transcription templates revealed the periodic spacing of nucleosomes in chromatin assembled with either wt H4 or H4K12su octamers, clearly indicating that H4K12su does not inhibit the formation of recombinant chromatin (Figure 2B). In this background, addition of the transcription activator Gal4-VP16, p300, acetyl-CoA, [α-^{32}P]-CTP, rNTPs, and transcriptional machinery from a HeLa nuclear extract resulted in the transcription of a 365 base RNA from the chromatin template assembled with wt H4 histones (Figure 2C). Surprisingly, and in contrast to the direct structural decompaction

of chromatin by H4K12su, transcription from templates assembled with H4K12su was drastically inhibited when compared with templates assembled with wt H4. The addition of Trichostatin A (TSA), a nanomolar inhibitor of class I and II HDACs, did not lead to significant changes in transcription, indicating that the repressive effect of H4 K12su is not significantly mediated through HDAC1 in chromatinized templates assembled with non-acetylated histones.[33] Importantly, our results unambiguously demonstrated transcriptional repression when site-specifically sumoylated H4 was present in chromatin.

H4 acetylation is inhibited prior to gene transcription in chromatin containing H4K12su. Based on our observations with sumoylated octamer and nucleosome substrates, we wondered if the inhibition of transcription by H4K12su also correlated with diminished H4 tail acetylation by p300. Previous in vitro transcription studies with chromatinized plasmids containing either K-to-R mutations in the H4 tail or truncated H4 missing tail residues 1-19 revealed an ~80 % reduced transcriptional output relative to transcription from chromatin containing wt H4.[20] Chromatinized plasmids containing either wt H4 or H4K12su were incubated with Gal4-VP16, p300 and acetyl-CoA for 30 min to enable steps preceding transcription; and the histones were subsequently resolved by SDS-PAGE and analyzed by tandem mass spectrometry after chemical propionylation, trypsination, and separation by capillary-liquid chromatography (Figure S3).[34] A critical innovation in the bottom-up analysis workflow was our use of the SENP2 catalytic domain to desumoylate H4K12su within the polyacrylamide gel matrix after SDS-PAGE. This procedural step was important to generate the same H4(4-17) tryptic peptide from wt H4 and H4K12su after p300-mediated acetylation. The H4(4-17) peptide contains K5,8,12 and 16 that are known to be acetylated by p300 in vitro and in vivo.[30]

Analysis of the H4(4-17) tryptic peptides arising from wt H4 revealed a remarkable degree of hyperacetylation within 30 min. The most abundant peptide corresponded to the K5,8,12,16 tetra-acetylated form with some tri-acetylated species also present (Figure 3A, Table 1, and Figures S4-S5). This is consistent with the fact that p300 acetylates histones to facilitate transcription.[20-22, 27] No significant degree of monoacetylation was observed, and a low abundance of diacetylated peptide was detected after manually searching the MS-MS spectra over the expected elution time (Figure S6). In comparison, chromatin assembled with H4K12su generated significantly fewer hyperacetylated peptides, with approximately equal amounts of tri- and di-acetylated H4(4-17) peptides (Figures 3B and Figures S7-S8). Small amounts of unmodified H4(4-17) peptides were also observed (Figure S9). This clearly indicates that H4K12su directly inhibits p300-mediated H4 tail acetylation in the steps prior to transcription. Given the importance of H4 tail acetylation for efficient transcription, H4K12su likely inhibits transcription, in-part, by directly inhibiting p300 activity on H4.

Since all four acetylated states of H4(4-17) were observed during tandem-MS-based analysis of p300 assay products with octameric and chromatin substrates, we interrogated the site-specificity of p300 in the H4 tail. Consistent with previous reports, we observed that K5 and K8 are preferred sites in the double acetylated H4 tail, over acetylation at K12 and K16 (Table 2).[35] Additionally, K12 was preferentially acetylated over K16 in the triply acetylated H4 tail peptide (Table 3). These observations were consistent between H4 or H4K12su containing substrates, indicating that the intrinsic substrate preference of p300 is unchanged in the presence of SUMO-3 (Table 4).

H3K4 methylation by COMPASS is inhibited in nucleosomes containing H4K12su. Along with H4K16ac, trimethylation at Lys 4 in histone H3 (H3K4me3) is a key mark associated with active

gene transcription.[36] In humans, H3K4me3 is installed by the SETD1A/B and MLL-1/2 enzyme complexes, while the corresponding yeast enzyme complex is COMPASS (Complex of proteins associated with Set1).[37] Importantly, the catalytic module that imparts enzymatic activity and product specificity is evolutionarily conserved in animals and yeast, and consists of Set1 and the subunits Swd1, Bre2, Swd3 and Sdc1 in COMPASS. In an effort to understand the mechanism of auto-regulation in SET1/MLL enzymatic complexes, we recently reported the reconstitution and structural characterization of an extended catalytic module (eCM) of COMPASS that contains both the nSET domain of Set1 and the Spp1 subunit (Figure 4A).[24] Although ubiquitylation at H2BK120 stimulates the methyltransferase activity of the eCM, it is not absolutely critical for nucleosome methylation by SET1/COMPASS complexes in vitro.[38] Based on our previous observation that H4K12su biochemically opposes the presence of H3K4me2 in nucleosomes by stimulating the activity of the H3K4me1/2 demethylase LSD1, we asked if H4K12su also directly opposes the installation of H3K4me3 in nucleosomes. Recent cryo-EM structures of the COMPASS eCM bound to the nucleosome core particle show significant spatial separation between the disordered H4 tail and the eCM (Figure 4A), thereby making it hard to predict any biochemical crosstalk between sumoylation and methylation.[24, 39] In order to shed light on this problem, methylation assays were undertaken with mononucleosome substrates containing either wt H4 or H4K12su and the six-subunit eCM (Figure S10). The degree of H3K4me1/2/3 was measured by Western blot with antibodies specific for the different H3 methylation states (Figure 4B). These experiments clearly showed that H4K12su inhibits the installation of H3K4me1/2/3 on nucleosomes. Moreover, the negative biochemical crosstalk arises from the presence of the Spp1 subunit in the eCM, because the core 5 protein catalytic module (Set1, Swd1, Bre2, Swd3, Sdc1) remained active on nucleosomes with or without the presence of H4K12su (Figure 4C). Thus, we

conclude that H4K12su in nucleosomes engages in negative biochemical crosstalk with p300-mediated acetylation within the same H4 tail, in *cis*, and may engage in negative biochemical crosstalk with the COMPASS-mediated methylation in the H3 tail, in *trans*.

Discussion

Histone marks in eukaryotic chromatin represent a range of biological pathways that modulate chromatin structure and function.[40] Marks may directly alter chromatin structure either through their steric bulk or by changing the charge of amino acid side-chains. Additionally, marks may recruit chromatin-modifying enzymes that change the modification state of other histones within a nucleosome. The biochemical crosstalk between marks is considered positive when one mark directs installation of another, and negative when one mark opposes the installation of another. The specific sumoylation of histones in chromatin was associated with the repression of gene transcription through early studies in yeast and human cells.[6, 14] We previously discovered the negative biochemical crosstalk between H4 sumoylation and H3K4me2 in nucleosomes mediated by the CoREST-LSD1 sub-complex, which suggested that sumoylation of actively transcribed regions enriched in H3K4me2 may lead to histone demethylation and silencing.[16] However, the direct effect of H4K12su in chromatin on p300-mediated gene transcription by RNAPII remained entirely unknown. Our semisynthesis of H4K12su using the ligation auxiliary, 2-aminooxyethanethiol, enabled the first interrogation of biochemical crosstalk between histone sumoylation and p300-catalyzed histone acetylation in reconstituted octamers, nucleosomes and chromatinized plasmids. Interestingly, we found that although H4K12su has no significant impact on the acetylation of other histones, in either histone octamer or nucleosomal contexts, it significantly impedes acetylation in the unstructured H4 N-terminal tail. While the simplest explanation is that steric bulk of the 93-amino acid SUMO-3 at K12 prevents acetylation at

proximal lysines, this should not be taken for granted as ubiquitin-family modifications at lysines do not always occlude enzymatic activity at proximal sites. For example, the ubiquitylation at K119 in the H2A C-terminus by the polycomb repressive complex 1 (PRC1) E3 ligases Ring1B/Bmi1 does not inhibit ubiquitylation at K124/K127/K129 in the H2A tail by the BRCA1-BARD1 heterodimeric E3 ligase.[41] Therefore, reduced acetylation may equally arise from a specific spatial orientation of the H4 tail upon its sumoylation that limits access to the p300 active site.

Given the essential role of acetylated lysines in the H4 tail on chromatin structure and gene transcription in vitro and in cells,[20] we surmised that diminished H4 acetylation may adversely influence gene transcription. Surprisingly, replacing wt H4 with H4K12su had no significant effect on the efficiency of plasmid chromatinization by the histone chaperone Nap1 and remodelers ACF1 and ISWI, resulting in regularly positioned nucleosomes for both wt H4 and H4K12su. Notably, however, an analysis of these chromatinized plasmid substrates in activator-and p300-dependent transcription assays with nuclear extracts revealed a strong repression of transcription by H4K12su. Toward a further understanding of the H4 acetylation events whose loss leads to this repression, bottom-up mass spectral analysis with data-independent acquisition of tryptic H4 peptides after SDS-PAGE resolution of the transcription assay components demonstrated reduced acetylation in the H4(4-17) peptide when chromatin was reconstituted with H4K12su. To the best of our knowledge, this is the first mass-spectral analysis of acetylation in the tail of chromatin-associated H4 following in vitro transcription, and also the first demonstration that the catalytic domain of the SUMO-specific protease SENP2 can desumoylate histones in SDS-PAGE gels. Given the inherent challenges of detecting SUMO target sites in substrates, due to the lack of a convenient trypsin cleavage site at the C-terminus of SUMO, the ability to selectively remove

SUMO using SENP2 may be particularly useful for analyzing sumoylated proteins in complex mixtures that require some degree of separation by SDS-PAGE. The fact that chromatinized plasmids containing H2B ubiquitylated at K120 show similar levels of transcription to unmodified chromatin suggests that the inhibition of transcription we observed may not strictly be due to the steric bulk of SUMO in chromatin.[19]

In addition to histone acetylation, another key histone mark associated with active transcription and enriched at promoter regions is H3K4me3. Installed by the Set1 containing COMPASS complex in yeast and the SET1/MLL1-4 family of methyltransferases in humans, H3K4me3 activates transcription in p53- and p300-dependent transcription from chromatinized plasmids[38]. And although H2BK120ub stimulates the methylation of H3K4, it is not absolutely critical for SET1 complex activity.[38] Structures of the 5-protein core catalytic module of COMPASS[42] and the 6-protein extended catalytic module were recently reported.[24] While the CM complex does not change methyltransferase activity in the presence of H2BK120ub, the eCM demonstrates some activity on nucleosomes that is further enhanced by the presence of H2BK120ub.[24] Consistent with this observation, the human SET1 complex also retains some in vitro activity on chromatinized templates lacking H2BK120ub.[38] From the cryo-EM structure of the eCM complex bound to nucleosomes, and the relative position of the unstructured H4 tail (Figure 4A), we wondered if H4K12su would have an effect on H3K4me3 methylation by COMPASS. We discovered that although the CM is not hindered by the presence of H4K12su in nucleosomes, the eCM is significantly hindered by SUMO. From the differences in composition of the two subcomplexes, we propose that SUMO may sterically interact with the Spp1 subunit in the eCM and may reduce nucleosome binding and/or productive catalysis by the Set1 protein. Interestingly, our results from methyltransferase assays, in conjunction with previous observations

that H4 tail sumoylation inhibits chromatin compaction, appear to indicate that SUMO attached to the H4 tail does not extend away from the nucleosome, but instead may occupy a fixed space that prevents the close apposition of both adjacent nucleosomes and histone-modifying enzymes in chromatin. Future structural studies will aim to identify the precise placement of SUMO in sumoylated nucleosomes. As histone acetylation by p300 also stimulates SETD1 activity on chromatin, the direct effect of H4K12su on p300-stimulated SETD1 methylation at H3K4 remains an interesting question.[38]

Collectively, the disruption of H4 tail acetylation and H3 tail methylation by the presence of H4K12su along with the inhibition of p300-mediated transcription from chromatinized templates have revealed multiple biochemical pathways by which histone sumoylation may inhibit gene transcription (Figure 5). These results have shed light on important aspects of chromatin regulation by histone H4 sumoylation and provide a strong mechanistic basis for the proposed roles for SUMO from studies in yeast and cultured human cells.

Materials and Methods

Key Resources Table

Resource or Reagent	Source	Identifier
acetyl-CoA	Roche	10101893001
Calcium Phosphate Transfection Kit	Thermo	K278001
Anti-DYKDDDDK G1 Affinity Resin	GenScript	L00432
HisPur Ni-NTA resin	Thermo	88221
[^{3}H]-acetyl-CoA	American Radiolabeled Chemicals	ART0213B
Pierce Trypsin Protease, MS Grade	Thermo	90057
Propionic anhydride	Sigma Aldrich	P51478
DMEM	Gibco	11956118
DPBS	Gibco	14190250
Fetal bovine serum	Gibco	16000044
Amplify fluorographic reagent	GE Amersham	NAMP100

Kodak GBX developer and fixer	Carestream Health	1900943
Trifluoroacetic acid	Alfa Aesar	AA31771-36
Formic Acid	Acros Organics	AC147932500
Acetonitrile (ACN)	Fisher	A996
C18 Zip tip	Millipore	ZTC18S096
Glacial acetic acid	Fisher	A38C-212
Bacterial Strains	Source	Identifier
E. coli BL21(DE3) competent cells	Thermo	FEREC0114
E. coli DH5α competent cells	NEB	C2987HVIAL
Plasmids	Source	Identifier
pST100-20xNCP*601*a	Gift from Dr. Robert K. McGinty	
pcDNA3.1-p300-His_6	Addgene	23252
pET28a-His_6-SENP2(365-590)	Addgene	16357
Primers	Source	Identifier
5'-ATCCTTGTAATCGTGTATGTCTAGTGTACTC-3'	IDT	p300_Ctrm_FLAG_R
5'-GATGACGATAAATAGTGATACTAAGCTTAAGTTTAAAC-3'	IDT	p300_Ctrm_FLAG_F
Antibodies	Source	Identifier
Polyclonal anti-acetyllysine antibody	Millipore	AB3879
Polyclonal anti-H4K16ac antibody	Active Motif	39167
Monoclonal anti-H3K4me1	Cell Signaling Technology	5326
Polyclonal anti-H3K4me2	Abcam	ab7766
Polyclonal anti-H3K4me3	Abcam	ab8580
Polyclonal anti-Histone H3	Abcam	ab1791
anti-rabbit, HRP conjugated	GE Healthcare	NA934
IRDye 800CW Goat anti-Rabbit IgG	Li-COR Biosciences	926-32211
IRDye 800CW Goat anti-Mouse IgG	Li-COR Biosciences	926-32210

HPLC purification

Proteins and peptides were analyzed (4.6 x 150 mm, 5 µm) and purified (22 x 250 mm, 15 - 20 µm) with C4 and C18 reverse-phase HPLC columns from Vydac (Deerfiled, IL) on either a Varian Prostar (Palo Alto, CA) or Agilent (Santa Clara, CA) 1260 Infinity II LC system. The mobile phase consisted of Buffer A (0.1% trifluoracetic acid in water), and Buffer B (90% acetonitrile in water, 0.1% trifluoroacetic acid). UV-vis profiles of eluting peptides/proteins were monitored at 214 and 280 nm.

Electrospray ionization mass spectrometry

Routine peptide/protein mass spectrometry was performed by direct infusion on a Bruker (Billerica, MA) Esquire ion-trap mass spectrometer operating in positive mode.

Recombinant human histone purification

Human histones H2A 2-A, H2B 1-K, H3.2, and H4 were expressed from pET3a plasmids in *E. coli* BL21(DE3) cells.[15] The insoluble histones were extracted from exclusion bodies with 6 M Gn-HCl, 10 mM Tris, pH 7.5. Histones were precipitated by dialysis against Millipore water in Spectra/Por 6 3.5 kDa molecular weight cut-off dialysis tubing and lyophilized to dryness. Crude histones were dissolved in 6 M Gn-HCl and purified by preparative C4 RP-HPLC.

Semisynthesis of H4K12su

The peptide H4(1-14)K12ivDde-C(O)$NHNH_2$ was synthesized on 2-chlorotrityl chloride resin by standard 9-fluorenylmethoxycarbonyl (Fmoc)-based solid phase peptide synthesis on a CEM Liberty Blue Automated Microwave Peptide Synthesizer (Matthews, NC).[16] The protected ligation auxiliary, *O*-(2-(tritylthio)ethyl)hydroxylamine, was incorporated at K12 by coupling bromoacetic acid at deprotected K12 on the resin followed by displacement of the bromide with 0.25 M auxiliary in dry DMSO. After acidolytic cleavage from the resin and C18 RP-HPLC purification, the H4(1-14)K12aux-C(O)$NHNH_2$ peptide (6 equivalents) was ligated with purified SUMO-3(2-91)C47S-MESNa thioester (1 equivalent) in ligation buffer consisting of 6 M Gn-HCl, 100 mM Na_2HPO_4, pH 7.3 to generate H4(1-14)K12su(aux)-C(O)$NHNH_2$ after 24 h at 25 °C. After C18 RP-HPLC purification, the sumoylated H4(1-14) peptidyl hydrazide was converted to the C-

terminal acyl azide by diazotization with 15 equivalents of $NaNO_2$ in 200 mM Na_2HPO_4, 6 M Gn-HCl, pH 3.0 at -20 °C for 20 min. The acyl azide was converted to the 4-mercaptophenylacetic acid (MPAA) C-terminal α-thioester in situ and ligated with purified H4(15-102)A15C truncant protein (2 equivalents) in a ligation buffer consisting of 200 mM Na_2HPO_4, 6 M Gn-HCl, 200 mM MPAA, pH 6.5. The pH was adjusted to 6.8-7.0 and ligation allowed to proceed at 25 °C for 24 h. The full length H4(A15C)K12su(aux) ligation product was purified by C4 RP-HPLC and the ligation auxiliary subsequently cleaved by activated Zn in 6 M Gn-HCl, pH 3.0, at 37 °C under argon over 24 h. This yielded pure H4(A15C)K12su after C4 RP-HPLC purification. Finally, radical mediated desulfurization of Cys15 to the native Ala15 in histone H4 was accomplished by first dissolving H4(A15C)K12su in 100 mM Na_2HPO_4, 6 M Gn-HCl, 500 mM TCEP, 100 mM MESNa, pH 7.5. To this solution was added 2-methyl-2-propanethiol to a concentration of 280 mM and the radical initiator 2,2'-Azobis[2-(2-imidazolin-2-yl)propane]dihydrochloride (VA-044) to a concentration of 10 mM. Desulfurization was allowed to proceed at 37 °C for 24 h and the final sumoylated histone product, H4K12su, was purified by C4 RP-HPLC.

147 bp Widom 601 DNA preparation

A plasmid containing 20 repeats of the 147 bp Widom 601 sequence, pST100-20xNCP601a was a kind gift from Professor Robert K. McGinty (UNC, Chapel Hill).[43] The plasmid was used to transform *E. coli* DH5α and propagated in LB media. The plasmid was extracted from cells by alkaline cell lysis and precipitated with isopropanol. The precipitate was collected by centrifugation and washed with 70% ethanol, followed by resuspension in 20 mM Tris, pH 8.0. The plasmid was purified by SOURCE 15Q 4.6/100 PE strong anion exchange column and analyzed by 1% agarose gel electrophoresis. Fractions pure from RNA contamination were pooled

and dialyzed against 10 mM tris, pH 8, overnight. The plasmid was cleaved by EcoRV to liberate the 147 bp 601 Widom sequence overnight. The plasmid backbone was separated by PEG precipitation followed by SOURCE 15Q 4.6/100 PE anion exchange. Pure fractions of 147 bp dsDNA, as seen by 1.5% agarose gel electrophoresis, were pooled and dialyzed against 10 mM Tris, pH 7.0, overnight and stored frozen at -20 ^{o}C.

Octamer and mononucleosome formation

All four histones were combined in equimolar amounts in 7 M Gn-HCl, 20 mM tris, pH 7.5 at a final concentration of 1 mg/mL and dialyzed against 10 mM Tris, 2 M NaCl, 1 mM EDTA, pH 7.5 overnight at 4 ^{o}C. The self-assembled crude octamers were purified by size-exclusion chromatography on a Superdex-200 10/300 GL column attached to an AKTA FPLC (GE Healthcare, Chicago, IL). Pure fractions were identified by 15% SDS-PAGE after coomassie staining. Pure octamer fractions were combined and concentrated, diluted with 10% glycerol and flash frozen for long-term storage. Mononucleosomes were formed by mixing equivalent amounts of histone octamers and 147 bp Widom *601* DNA in a buffer consisting of 2 M NaCl and 10 mM Tris, pH 7.0, followed by dialysis against 10 mM Tris to a final NaCl concentration of 200 mM. Small-scale mononucleosome formation tests were first undertaken to fine-tune the molar ratio of octamer to 147 bp DNA before large-scale preparations. This avoided the presence of unbound 147 bp DNA in the mononucleosome preparations as seen by 5% TBE gels stained with ethidium bromide. Freshly prepared mononucleosomes containing wt H4 or H4K12su were stored on ice at 4 °C for a maximum period of 3 weeks.[15]

Purification of the SENP2 catalytic domain

A pET28a plasmid containing the SENP2 catalytic domain (cat.SENP2) was obtained from Addgene (Catalog number 16357).[44] The protein was expressed and purified from *E. coli* (DE3) cells. Briefly, cells were grown in 2xYT medium at 37 °C until OD_{600} 0.6-0.8 and protein expression was induced with 0.5 mM isopropyl-*β*-D-galactopyranoside for 3 h at 25 °C. Cells were collected by centrifugation and lysed by sonication in 20% (w/v) sucrose, 20 mM Tris, 350 mM NaCl, 20 mM imidazole, 1 mM *β*-mercaptoethanol, 1 mM phenylmethylsulfonyl fluoride (PMSF), pH 8.0. The lysate was clarified by centrifugation and bound to Ni^{2+}-NTA resin over 1 h with continuous nutation at 4 °C. The resin was then washed with a buffer containing 20 mM Tris, 350 mM NaCl, pH 8.0, followed by successive buffers containing increasing amounts of imidazole from 20 mM to 100 mM to elute non-specifically bound proteins. Finally, the cat.SENP2 was eluted with a buffer containing 20 mM Tris, 350 mM NaCl, 400 mM imidazole, pH 8.0. Fractions containing cat.SENP2 were identified by 15% SDS-PAGE, pooled and dialyzed in Spectra/Por 6 dialysis tubing with 15 kDa molecular-weight cut-off against 2 L of dialysis buffer containing 20 mM Tris, 100 mM NaCl, 5% (v/v) glycerol, pH 8.0 at 4 °C for two hours, twice. The dialyzed protein was stored at -80 °C in aliquots flash frozen in liquid nitrogen.

DNA cloning and sequencing

A Q5 site-directed mutagenesis kit (NEB, Ipswitch, MA) was used to generate pcDNA3.1-p300-FLAG from the plasmid pcDNA3.1-p300-His_6 obtained from Addgene (Catalog number 23252) by following the manufacturer's protocols. Oligos for molecular cloning were purchased from Integrated DNA Technologies (Coralville, IA) and DNA sequencing was carried out by Eurofins Genomics (Louisville, KY).

Preparation of pcDNA for transfection

DNA for transient transfection was prepared by Miraprep of *E. coli* DH5α cells as previously described using a Qiagen (Valencia, CA) DNA miniprep kit.[45] Briefly, transformed *E. coli* DH5α cells were grown in 50 mL LB media supplemented with ampicillin (50 μg/mL) overnight at 37 °C. Cells were collected by centrifugation and resuspended in P1 buffer supplemented with fresh RNase. After alkaline lysis and neutralization, the supernatant was cleared by centrifugation. The supernatant was diluted with an equal volume of 96% (v/v) ethanol prior to loading onto five Qiagen miniprep spin columns. At this point, the DNA was washed and eluted according to the Qiagen protocol. Purity of the eluted DNA was checked by measuring the $A_{280\ nm}/A_{260\ nm}$ ratio on a NanoDrop 2000c spectrophotometer and by agarose gel electrophoresis. The correct gene sequence for p300 was also confirmed by sequencing prior to transfection in human cells.

HEK293T cell culture

HEK293T cells were cultured in T75 flasks using Dulbecco's Modified Eagle Medium supplemented with 10% fetal bovine serum and incubated at 37 °C in a 5% CO_2 atmosphere.

Transient transfection of HEK293T cells

HEK293T cells were cultured to ~60% confluency before transient transfection with pcDNA3.1-p300-FLAG. The cell growth medium was changed at least 1 h before transfection. Cells were transfected with the Calcium Phosphate Transfection Kit (Thermo Fisher Scientific, Waltham, MA) using 15 μg DNA per T75 flask. Cells were grown in transfection medium over 48 hours before detachment by trypsin and collection by centrifugation. The cell pellet was washed thrice

with ice-cold Dulbecco's Phosphate-buffered Saline before either protein purification or storage at -80 °C.

Purification of the full-length histone acetyltransferase p300.

The washed HEK293T cell pellet was resuspended in lysis buffer consisting of 20 mM Tris, pH 7.4 at 4 °C, 0.5 M KCl, 5 mM $MgCl_2$, 0.1% (v/v) IGEPAL CA-630, 1 mM PMSF, 1x EDTA-free protease inhibitor (Roche, Basel, CH), 10 % (v/v) glycerol then frozen in dry ice and allowed to thaw at room temperature. The lysate was nutated for 30 min at 4 °C before clarifying by centrifugation at 17,620*rcf* for 30 min at 4 °C. The soluble fraction was bound to anti-DYKDDDDK resin (Genscript, Piscataway, NJ) for 1 h at 4 °C, then washed four times in lysis buffer and finally once in lysis buffer containing 150 mM KCl without protease inhibitors. The full-length p300-FLAG protein was eluted with 200 µg/mL 3xFLAG peptide in 150 mM KCl containing lysis buffer. The purity and concentration of p300-FLAG were assessed by 8% SDS-PAGE using BSA standards (ThermoFisher) and by western blot with an anti-FLAG antibody (Sigma). Aliquots of p300-FLAG in 10% (v/v) glycerol containing elution buffer were flash frozen in liquid nitrogen and stored at -80 °C.

Histone acetylation assays

Histone acetylation assays were conducted as outlined in Figure S1B. In brief, 30 µL volume assays were prepared by mixing histone octamers (300 nM), acetyl-CoA (25 µM), and p300-FLAG (150 pM) in histone acetyltransferase buffer consisting of 50 mM Tris, pH 8.0, 1 mM DTT, 1 mM PMSF, 0.1 mM EDTA and 10% (v/v) glycerol. Acetylation assays with octamer substrates were undertaken at 30 °C for 30 min and stopped by heating the assay mixture to 65 °C for 10 min

which denatures p300. For fluorography, 389 nM mononucleosomes containing either H4 or H4K12su were incubated with 2 µL [^{3}H]-acetyl-CoA (15.95 Ci/mmol) and p300 (292 pM) overnight at 30 °C before heat denaturation at 65 °C for 10 min.[46] Heat denatured samples were cooled down to 30 °C before the addition of cat.SENP2 (3 equivalents relative to H4K12su). To ensure similar sample handling, cat.SENP2 was added to both H4 and H4K12su assay samples. After 2 h of desumoylation with cat.SENP2, the samples were denatured with 6xLaemmli and resolved by SDS-PAGE prior to analysis by western blotting or by fluorography.

Histone methyltransferase assays

Nucleosome (0.5 µM) and COMPASS CM or COMPASS eCM (1 µM) were incubated together in 20 mM HEPES, pH 7.5, 100 mM NaCl, 1 mM DTT, 0.2 mM SAM for 30 min at 30 °C. The reaction was quenched in SDS-PAGE loading buffer and analyzed by western blot.[24]

Western blots

Western blots were performed in modified Towbin buffer consisting of 25 mM Tris, 192 mM glycine, 2 mM SDS, 10% (v/v) methanol, and proteins were transferred onto PVDF membrane at 90 V overnight. Membranes were blocked in 5% (w/v) non-fat milk powder in phosphate-buffered saline (PBS) for 1 h at 25 °C before incubating overnight in diluted primary antibody in 5% (w/v) non-fat milk powder in PBST (PBS containing 0.05% (v/v) Tween-20) at 4 °C. Overnight incubated membranes were washed in PBST before incubating with IR-dye conjugated secondary antibody or HRP-conjugated secondary antibody in 5% (w/v) non-fat milk powder containing PBST for 1 h at 25°C. After incubation with secondary antibodies, the membranes were washed

first in PBST and then PBS before scanning on a Li-COR Biosciences (Lincoln, NE) Odyssey IR scanner or developing with ECL reagents.

Fluorography

After SDS-PAGE separation of methylation assay components, gels were soaked in Amplify solution (GE Healthcare, Chicago, IL) for 30 min before drying on a vacuum air dryer. Dried gels were exposed to X-ray film for 1 week at -80 °C. Images were developed and fixed using Kodak (Rochester, NY) GBX solutions.

Chromatin assembly and MNase digestion

Chromatin assembly and micrococcal nuclease analysis proceeded essentially as described previously.[22] Briefly, octamer and hNAP-1 were incubated together on ice for 15 min before the addition of hTopo1, dACF1/ISWI, relaxed circular plasmid DNA, and ATP-Mg mix (0.5 M creatine phosphate, 0.5 M ATP, 1 M $MgCl_2$, 5 mg/mL creatine kinase) and incubated at 30 °C for 2 h. Micrococcal nuclease (TaKaRa Bio Inc., Shiga, JP) was added to chromatin and digested at 25 °C for 10 min. DNA was purified from the digested chromatin by miniprep kit and analyzed by 1.25% agarose gel stained with ethidium bromide.

In vitro transcription assay

Assays were conducted as outlined in Figure 2A following previously described protocols.[22, 47] Gal4-VP16 (30 ng), chromatin template (25 ng), p300 (10 ng), and acetyl-CoA (5 μM) were incubated in 20 mM HEPES-KOH, pH 7.9, 1 mM EDTA, 100 mM KCl, 10% (v/v) glycerol, 0.2 mg/mL BSA at 30 °C for 10 min. Preinitiation complex formation was initiated by the addition of

HeLa extract (30 µg total protein) with continued incubation at 30 °C for 10 min. Transcription was initiated by the addition of ATP, UTP, CTP, 3'-O-methyl-GTP, and [α-^{32}P]-CTP followed by incubation at 30 °C for 1 h. Assay products were resolved by agarose gel and analyzed by autoradiography.

In-gel desumoylation and propionylation of lysine residues

Histone modification analysis by mass spectrometry was conducted as previously described with one key modification.[34] Histones were separated by SDS-PAGE and stained in coomassie stain consisting of 0.05% (w/v) Coomassie brilliant blue dissolved in 45:45:10 (v/v) methanol/H_2O/acetic acid. Bands were mostly destained in 45:45:10 (v/v) methanol/H_2O/acetic acid and specific histone bands were excised from the gel and diced into 1 mm cubes. Gel pieces were sequentially washed in 100 mM NH_4HCO_3, pH 8.0, and then dehydrated in sufficient acetonitrile to cover the gel pieces with gentle agitation for 15 min at 25 °C. Gel pieces were dried by lyophilization before rehydrating in the presence of cat.SENP2 (1 µg/µL) in histone acetyltransferase assay buffer on ice for 30 min, and further incubated overnight at 30 °C. After desumoylation, the gel pieces were sequentially washed in 100 mM NH_4HCO_3, pH 8.0, and then dehydrated in sufficient acetonitrile to cover the gel pieces with gentle agitation for 15 min at 25 °C. Histones were propionylated in-gel with 1:2 (v/v) 100 mM NH_4HCO_3/propionic anhydride for 20 min with shaking at 25 °C. The propionylation reagent was aspirated away from gel pieces and they were sequentially washed in 100 mM NH_4HCO_3, pH 8.0, and then dehydrated in sufficient acetonitrile to cover the gel pieces with gentle agitation for 15 min at 25 °C. In-gel propionylation was undertaken thrice to ensure complete reaction.

In-gel tryptic digestion and peptide extraction

Histones were digested by rehydrating gel pieces with 12.5 ng/µL trypsin (Pierce) in 50 mM NH_4HCO_3 on ice for 30 min, and then incubation at 30 °C overnight. The bicarbonate solution after overnight digestion contained histone peptides that were transferred into a new empty tube. Peptides were further extracted from the trypsinized gel pieces by the sequential addition of 20 µL milliQ pure H_2O and shaking for 15 min, followed by incubation with 20 µL acetonitrile and shaking for 15 min. All three solutions – bicarbonate, water and acetonitrile – were pooled together. The peptide extraction process was repeated once and the combined peptide solutions were lyophilized to dryness. The dry tryptic peptides were propionylated to cap newly formed N-termini by resuspending in 30 µL 100 mM NH_4HCO_3 and adjusting to pH 8.0 before the addition of 15 µL 1:3 (v/v) propionic anhydride:ACN. The pH was quickly readjusted to pH 8.0 with NH_4OH before shaking for 15 min at 25 ºC. The reaction mixture was dried on the lyophilizer and the propionylation of N-termini was repeated once to ensure complete reaction.

C18 Zip-tip desalting of histone peptides

The dried histone peptides were dissolved in 50 µL 0.1 % (v/v) TFA in milliQ pure H_2O by vortexing and sonication in a water-bath, and the pH was adjusted to ~ 4.0 with TFA prior to desalting with C18 Zip-tips (EMD Millipore). The Zip-tip was first washed sequentially with 3x10 µL acetonitrile and then washed with 3x10 µL 0.1% (v/v) aqueous TFA. Peptides were bound to the resin by pipetting the peptide solution through the Zip-tip resin in 10 µL aliquots until all the solution had passed through the resin at least once. The Zip-tip resin was then washed by stepwise transfer of 5x10 µL of 0.1 % (v/v) aqueous TFA into waste. The solid-phase bound peptides were then eluted into a clean empty tube by the stepwise transfer of 5x10 µL of 75% (v/v) acetonitrile

in water containing 0.5% (v/v) acetic acid. The combined eluted peptide solutions were lyophilized to dryness.

Nano-LC and tandem mass spectrometry analysis of histone peptides

The lyophilized histone tryptic peptides were dissolved in 15 µL of 10% (v/v) acetonitrile and 1% (v/v) formic acid in milliQ pure water by vortexing and sonication in a water-bath. Samples were loaded onto a C18 trap column (LC Packing) and then into a capillary column using an Agilent 1100 Series capillary LC system (Santa Clara, CA). The capillary column was packed in house with Phenomenex C12 Jupiter resin. The mobile phase used consisted of A (0.6% (v/v) acetic acid in milliQ pure water) and B (0.6% (v/v) acetic acid in acetonitrile). Peptides were separated over a 70 min gradient from 2% to 98% buffer B, and directly eluted through the nano electrospray ionization source into a Thermo Finnigan LTQ XL mass spectrometer (San Jose, CA) for MS and MS-MS analysis. Peptide ions were identified and analyzed manually using the Thermo Xcalibur Qual Browser. Precursor fragments were identified over at least two peptide spectra, when possible, with an error of ± 0.8 Da. Mass spectrometer parameters were: Isolation width: 1 m/z; normalized collision energy: 35.0; scan range m/z: 300.00–2000.00. Dynamic exclusion was enabled.

Acknowledgements

The authors thank the Departments of Chemistry and Pharmacology at the University of Washington and The Rockefeller University for generous support. Ning Zheng is an Investigator of the Howard Hughes Medical Institute. This research was supported by funding from NIH grants to C.C. (R01GM110430), N.Z. (R01HD097408) and R.G.R. (R01CA234561 and R01DK071900). C.A.L. was supported by a Molecular Biophysics Training Grant T32GM008268. C.E.W. was

supported by an ARCS Foundation Fellowship and an NSF Graduate Research Fellowship (grant number DGH-1256082).

References

[1] Kouzarides, T. (2007) Chromatin modifications and their function, *Cell 128*, 693-705.
[2] Strahl, B. D., and Allis, C. D. (2000) The language of covalent histone modifications, *Nature 403*, 41-45.
[3] Greer, E. L., and Shi, Y. (2012) Histone methylation: a dynamic mark in health, disease and inheritance, *Nat. Rev. Genetics 13*, 343-357.
[4] Shahbazian, M. D., and Grunstein, M. (2007) Functions of site-specific histone acetylation and deacetylation, *Annu. Rev. Biochem. 76*, 75-100.
[5] Weake, V. M., and Workman, J. L. (2008) Histone ubiquitination: triggering gene activity, *Mol. Cell 29*, 653-663.
[6] Shiio, Y., and Eisenman, R. N. (2003) Histone sumoylation is associated with transcriptional repression, *Proc. Natl. Acad. Sci. U.S.A. 100*, 13225-13230.
[7] Ryu, H. Y., Su, D., Wilson-Eisele, N. R., Zhao, D., Lopez-Giraldez, F., and Hochstrasser, M. (2019) The Ulp2 SUMO protease promotes transcription elongation through regulation of histone sumoylation, *EMBO J. 38*, e102003.
[8] Issar, N., Roux, E., Mattei, D., and Scherf, A. (2008) Identification of a novel post-translational modification in Plasmodium falciparum: protein sumoylation in different cellular compartments, *Cell. Microbiol. 10*, 1999-2011.
[9] Miller, M. J., Barrett-Wilt, G. A., Hua, Z., and Vierstra, R. D. (2010) Proteomic analyses identify a diverse array of nuclear processes affected by small ubiquitin-like modifier conjugation in Arabidopsis, *Proc. Natl. Acad. Sci. U.S.A. 107*, 16512-16517.
[10] Hendriks, I. A., and Vertegaal, A. C. O. (2016) A comprehensive compilation of SUMO proteomics, *Nat. Rev. Mol. Cell Biol. 17*, 581-595.
[11] Ohkuni, K., Takahashi, Y., Fulp, A., Lawrimore, J., Au, W. C., Pasupala, N., Levy-Myers, R., Warren, J., Strunnikov, A., Baker, R. E., Kerscher, O., Bloom, K., and Basrai, M. A. (2016) SUMO-targeted ubiquitin ligase (STUbL) Slx5 regulates proteolysis of centromeric histone H3 variant Cse4 and prevents its mislocalization to euchromatin, *Mol. Biol. Cell 27*, 1500-1510.
[12] Galisson, F., Mahrouche, L., Courcelles, M., Bonneil, E., Meloche, S., Chelbi-Alix, M. K., and Thibault, P. (2011) A novel proteomics approach to identify SUMOylated proteins and their modification sites in human cells, *Mol. Cell. Proteomics 10*, M110.004796.
[13] Hendriks, I. A., D'Souza, R. C., Yang, B., Verlaan-de Vries, M., Mann, M., and Vertegaal, A. C. (2014) Uncovering global SUMOylation signaling networks in a site-specific manner, *Nat. Struct. Mol. Biol. 21*, 927-936.
[14] Nathan, D., Ingvarsdottir, K., Sterner, D. E., Bylebyl, G. R., Dokmanovic, M., Dorsey, J. A., Whelan, K. A., Krsmanovic, M., Lane, W. S., Meluh, P. B., Johnson, E. S., and Berger, S. L. (2006) Histone sumoylation is a negative regulator in Saccharomyces cerevisiae and shows dynamic interplay with positive-acting histone modifications, *Genes Dev. 20*, 966-976.

[15] Dhall, A., Wei, S., Fierz, B., Woodcock, C. L., Lee, T. H., and Chatterjee, C. (2014) Sumoylated human histone H4 prevents chromatin compaction by inhibiting long-range internucleosomal interactions, *J. Biol. Chem. 289*, 33827-33837.

[16] Dhall, A., Weller, C. E., Chu, A., Shelton, P. M. M., and Chatterjee, C. (2017) Chemically Sumoylated Histone H4 Stimulates Intranucleosomal Demethylation by the LSD1-CoREST Complex, *ACS Chem. Biol. 12*, 2275-2280.

[17] Dignam, J. D., Lebovitz, R. M., and Roeder, R. G. (1983) Accurate transcription initiation by RNA polymerase II in a soluble extract from isolated mammalian nuclei, *Nucleic Acids Res. 11*, 1475-1489.

[18] Roeder, R. G. (2019) 50+ years of eukaryotic transcription: an expanding universe of factors and mechanisms, *Nat. Struct. Mol. Biol. 26*, 783-791.

[19] Kim, J., Guermah, M., McGinty, R. K., Lee, J. S., Tang, Z., Milne, T. A., Shilatifard, A., Muir, T. W., and Roeder, R. G. (2009) RAD6-Mediated transcription-coupled H2B ubiquitylation directly stimulates H3K4 methylation in human cells, *Cell 137*, 459-471.

[20] An, W., Palhan, V. B., Karymov, M. A., Leuba, S. H., and Roeder, R. G. (2002) Selective requirements for histone H3 and H4 N termini in p300-dependent transcriptional activation from chromatin, *Mol. Cell 9*, 811-821.

[21] Robinson, P. J., An, W., Routh, A., Martino, F., Chapman, L., Roeder, R. G., and Rhodes, D. (2008) 30 nm chromatin fibre decompaction requires both H4-K16 acetylation and linker histone eviction, *J. Mol. Biol. 381*, 816-825.

[22] Shimada, M., Chen, W. Y., Nakadai, T., Onikubo, T., Guermah, M., Rhodes, D., and Roeder, R. G. (2019) Gene-Specific H1 Eviction through a Transcriptional Activator-->p300-->NAP1-->H1 Pathway, *Mol. Cell 74*, 268-283 e265.

[23] Weller, C. E., Huang, W., and Chatterjee, C. (2014) Facile synthesis of native and protease-resistant ubiquitylated peptides, *ChemBioChem 15*, 1263-1267.

[24] Hsu, P. L., Shi, H., Leonen, C., Kang, J., Chatterjee, C., and Zheng, N. (2019) Structural Basis of H2B Ubiquitination-Dependent H3K4 Methylation by COMPASS, *Mol. Cell 76*, 712-723 e714.

[25] Ryu, H. Y., Zhao, D., Li, J., Su, D., and Hochstrasser, M. (2020) Histone sumoylation promotes Set3 histone-deacetylase complex-mediated transcriptional regulation, *Nucleic Acids Res. 48*, 12151-12168.

[26] Kraus, W. L., and Kadonaga, J. T. (1998) p300 and estrogen receptor cooperatively activate transcription via differential enhancement of initiation and reinitiation, *Genes Dev. 12*, 331-342.

[27] Kundu, T. K., Palhan, V. B., Wang, Z., An, W., Cole, P. A., and Roeder, R. G. (2000) Activator-dependent transcription from chromatin in vitro involving targeted histone acetylation by p300, *Mol. Cell 6*, 551-561.

[28] Mikolajczyk, J., Drag, M., Békés, M., Cao, J. T., Ronai, Z. a. e., and Salvesen, G. S. (2007) Small ubiquitin-related modifier (SUMO)-specific proteases: profiling the specificities and activities of human SENPs, *J. Biol. Chem. 282*, 26217-26224.

[29] Chen, L. F., Mu, Y., and Greene, W. C. (2002) Acetylation of RelA at discrete sites regulates distinct nuclear functions of NF-kappaB, *EMBO J. 21*, 6539-6548.

[30] Ogryzko, V. V., Schiltz, R. L., Russanova, V., Howard, B. H., and Nakatani, Y. (1996) The transcriptional coactivators p300 and CBP are histone acetyltransferases, *Cell 87*, 953-959.

[31] Akhtar, A., and Becker, P. B. (2000) Activation of transcription through histone H4 acetylation by MOF, an acetyltransferase essential for dosage compensation in Drosophila, *Mol. Cell 5*, 367-375.

[32] Shogren-Knaak, M., Ishii, H., Sun, J.-M., Pazin, M. J., Davie, J. R., and Peterson, C. L. (2006) Histone H4-K16 acetylation controls chromatin structure and protein interactions, *Science 311*, 844-847.

[33] Schultz, B. E., Misialek, S., Wu, J., Tang, J., Conn, M. T., Tahilramani, R., and Wong, L. (2004) Kinetics and comparative reactivity of human class I and class IIb histone deacetylases, *Biochemistry 43*, 11083-11091.

[34] Sidoli, S., and Garcia, B. A. (2017) Characterization of Individual Histone Posttranslational Modifications and Their Combinatorial Patterns by Mass Spectrometry-Based Proteomics Strategies, *Methods Mol. Biol. 1528*, 121-148.

[35] Schiltz, R. L., Mizzen, C. A., Vassilev, A., Cook, R. G., Allis, C. D., and Nakatani, Y. (1999) Overlapping but distinct patterns of histone acetylation by the human coactivators p300 and PCAF within nucleosomal substrates, *J. Biol. Chem. 274*, 1189-1192.

[36] Santos-Rosa, H., Schneider, R., Bannister, A. J., Sherriff, J., Bernstein, B. E., Emre, N. C. T., Schreiber, S. L., Mellor, J., and Kouzarides, T. (2002) Active genes are tri-methylated at K4 of histone H3, *Nature 419*, 407-411.

[37] Shilatifard, A. (2012) The COMPASS Family of Histone H3K4 Methylases: Mechanisms of Regulation in Development and Disease Pathogenesis, *Annu. Rev. Biochem. 81*, 65-95.

[38] Tang, Z., Chen, W. Y., Shimada, M., Nguyen, U. T., Kim, J., Sun, X. J., Sengoku, T., McGinty, R. K., Fernandez, J. P., Muir, T. W., and Roeder, R. G. (2013) SET1 and p300 act synergistically, through coupled histone modifications, in transcriptional activation by p53, *Cell 154*, 297-310.

[39] Worden, E. J., Zhang, X., and Wolberger, C. (2020) Structural basis for COMPASS recognition of an H2B-ubiquitinated nucleosome, *Elife 9, e53199*.

[40] Allis, C. D., Jenuwein, T., Reinberg, D., and Caparros, M.-L. (2007) *Epigenetics*, First ed., Cold Spring Harbor Laboratory Press, Cold Spring Harbor.

[41] Uckelmann, M., Densham, R. M., Baas, R., Winterwerp, H. H. K., Fish, A., Sixma, T. K., and Morris, J. R. (2018) USP48 restrains resection by site-specific cleavage of the BRCA1 ubiquitin mark from H2A, *Nat. Commun. 9*, 229.

[42] Hsu, P. L., Li, H., Lau, H. T., Leonen, C., Dhall, A., Ong, S. E., Chatterjee, C., and Zheng, N. (2018) Crystal Structure of the COMPASS H3K4 Methyltransferase Catalytic Module, *Cell 174*, 1106-1116.

[43] Dyer, P. N., Edayathumangalam, R. S., White, C. L., Bao, Y., Chakravarthy, S., Muthurajan, U. M., and Luger, K. (2004) Reconstitution of nucleosome core particles from recombinant histones and DNA, *Methods Enzymol. 375*, 23-44.

[44] Reverter, D., and Lima, C. D. (2009) Preparation of SUMO proteases and kinetic analysis using endogenous substrates, *Methods Mol. Biol. 497*, 225-239.

[45] Pronobis, M. I., Deuitch, N., and Peifer, M. (2016) The Miraprep: A Protocol that Uses a Miniprep Kit and Provides Maxiprep Yields, *PLoS One 11*, e0160509.

[46] Qiu, Y., Zhao, Y., Becker, M., John, S., Parekh, B. S., Huang, S., Hendarwanto, A., Martinez, E. D., Chen, Y., Lu, H., Adkins, N. L., Stavreva, D. A., Wiench, M., Georgel, P. T., Schiltz, R. L., and Hager, G. L. (2006) HDAC1 acetylation is linked to progressive modulation of steroid receptor-induced gene transcription, *Mol. Cell 22*, 669-679.

[47] An, W., and Roeder, R. G. (2004) Reconstitution and transcriptional analysis of chromatin in vitro, *Methods Enzymol. 377*, 460-474.

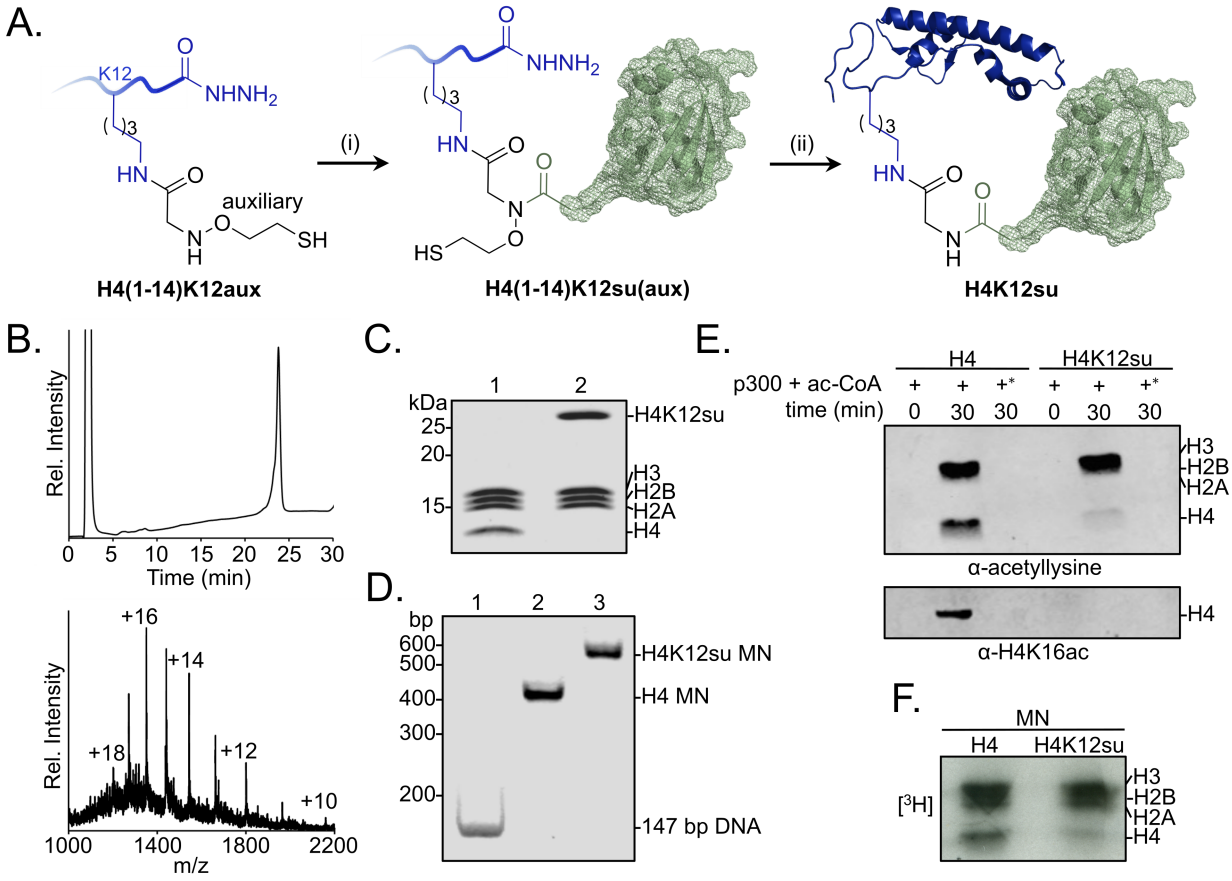

Figure 1. Sumoylation inhibits p300-mediated H4 acetylation in octamer and mononucleosome substrates. (A) Synthetic scheme for H4K12su. (i) An H4(1-14)K12aux peptide was ligated with a SUMO-3(2-91)C47S α-thioester. (ii) The sumoylated H4(1-14) peptidyl hydrazide containing the auxiliary was converted to a C-terminal α-thioester and ligated with H4(15-102)A15C. The auxiliary was then reductively cleaved from the ligation product. Cys15 in the final ligation product was desulfurized to the native Ala15 to yield site-specifically sumoylated H4K12su. (B) C4 analytical RP-HPLC trace of purified H4K12su (top). ESI-MS of purified H4K12su (bottom). Calculated mass 21,596.7 Da. Observed, 21,594.2 ± 3.4 Da. (C) Coomassie-stained 15% SDS-PAGE of reconstituted octamers containing wt H4 or H4K12su. (D) Ethidium bromide stained 5% TBE gel of mononucleosomes containing wt H4 or H4K12su. (E) Western blots of p300 assay products with octamer substrates containing wt H4 or H4K12su, probed with a site-independent pan-acetyllysine antibody (top) and an H4K16ac-specific antibody (bottom). An asterisk indicates assays with heat-inactivated p300 to exclude non-enzymatic acetylation. (F) Fluorogram of p300 assay products with [^{3}H]-acetyl-CoA as the co-factor and mononucleosome substrates containing wt H4 or H4K12su.

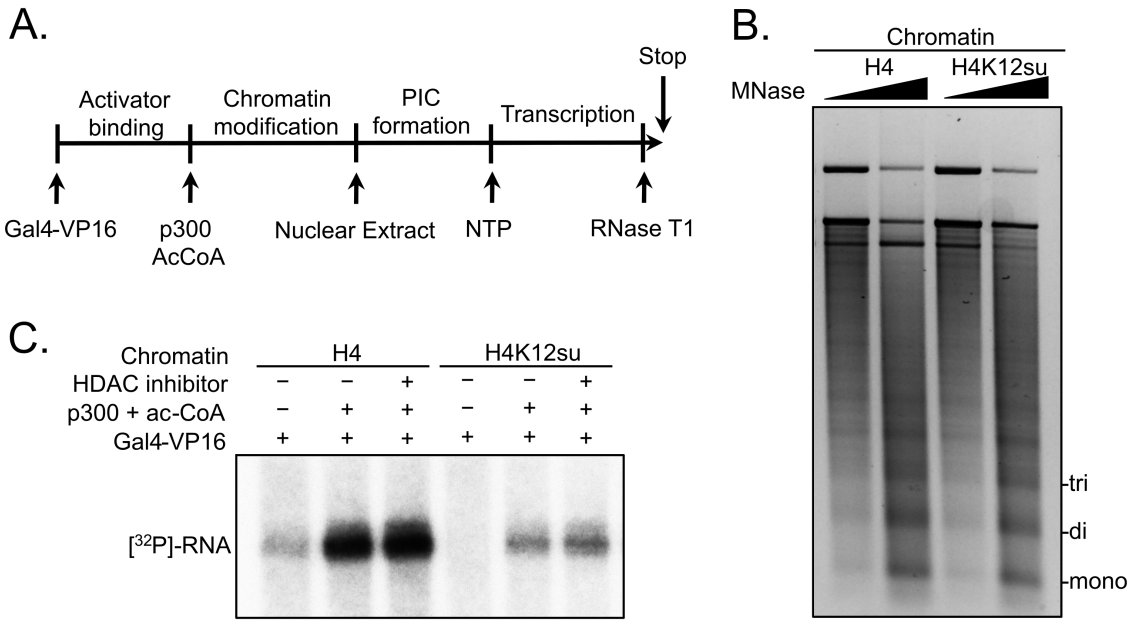

Figure 2. Histone H4 sumoylation inhibits in vitro transcription from chromatinized plasmid templates. (A) Scheme outlining steps during the in vitro transcription assay with chromatinized plasmids, nuclear extracts, activator Gal4-VP16 and p300. (B) Micrococcal nuclease digestion analysis of plasmids chromatinized with wt H4 or H4K12su indicating the similar occupancy and spacing of mononucleosomes. (C) Autoradiogram of ^{32}P-labeled 365-base RNA transcript generated from p300-mediated transcription from chromatinized templates containing wt H4 or H4K12su in the presence or absence of the HDAC inhibitor, Trichostatin A.

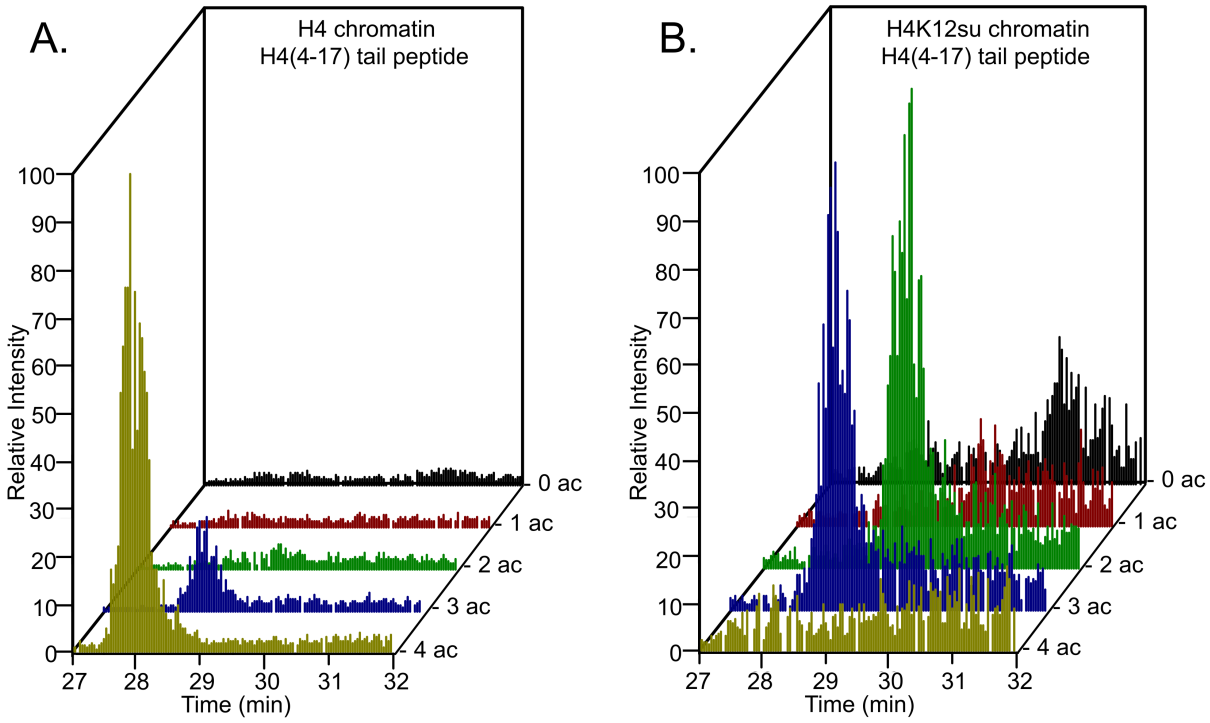

Figure 3. Comparison of H4 tail acetylation by p300 in chromatinized plasmid templates with activator Gal4-VP16. (A) Extracted ion chromatograms of all H4(4-17) tryptic peptides obtained after SDS-PAGE resolution and in-gel trypsination of acetylated chromatin containing wt H4. (B) Extracted ion chromatograms of all H4(4-17) tryptic peptides obtained after SDS-PAGE resolution, in-gel desumoylation and trypsination of acetylated chromatin containing H4K12su. The extracted m/z of each spectrum is centered on the $[M+2H]^{2+}$ precursor ion.

Table 1. H4(4-17) tail peptides acetylated by p300 in chromatinized plasmid templates with activator Gal4-VP16.[a,b]

H4(4-17) peptide	[M]	$[M+2H]^{2+}$	PSM H4	PSM H4K12su
prGKprGGKprGLGKprGGAKprR	1549.89	775.95	n.d.	1
prGKprGGKacGLGKprGGAKprR	1535.88	768.95	n.d.	n.d.
prGKacGGKacGLGKprGGAKprR	1521.86	761.94	2	3
prGKacGGKacGLGKacGGAKprR	1507.85	754.93	5	n.d.[c]
prGKacGGKacGLGKprGGAKacR	1507.85	754.93	n.d.	3[d]
prGKacGGKacGLGKacGGAKacR	1493.83	747.92	7	n.d.[c]

[a] Peptides were chemically propionylated before and after trypsinization to cap unmodified lysine side-chains and newly generated *N*-termini. [b] MS-MS spectra observed contained major fragments for the shown modification pattern over other potential patterns, however, no singly acetylated peptides were observed for wt H4. [c] Acetylation at K12 is not possible for H4K12su. [d] The triply acetylated peptide from H4K12su is blocked from acetylation at K12, but is propionylated after in-gel desumoylation. PSM= peptide spectral match. n.d. = not detected.

Table 2. Comparisons of relative ion-intensities of characteristic fragment-ions from an enzymatically di-acetylated and chemically propionylated H4(4-17) peptide, $[M+2H]^{2+}$ = 762 Da, after activator and p300-mediated acetylation of chromatinized plasmids containing wt H4.[a]

Species	Ion	% of Total ion intensity		Avg. ratio
K5ac, K8ac	b_5^+	1.316	1.654	12.4
K5pr, K8pr		0.072	0.253	
K12ac, K16ac	y_9^+	0.042	0.306	0.2
K12pr, K16pr		3.176	0.971	

[a] Only two unique spectra were observed and analyzed for the doubly acetylated and propionylated H4(4-17) tail peptide from wt H4 chromatin.

Table 3. Comparisons of relative ion-intensities of characteristic fragment-ions from an enzymatically tri-acetylated and chemically propionylated H4(4-17) peptide, $[M+2H]^{2+}$ = 755 Da, after activator and p300-mediated acetylation of chromatinized plasmids containing wt H4.[a]

Species	Ion	% of Total ion intensity			Avg. ratio
K5ac, K8ac, K12ac	b_9^+	3.032	4.938	3.981	24.1 ± 13.3
K5ac, K8ac, K12pr		0.339	0.096	0.147	
K5ac, K8ac, K12ac	b_{10}^+	0.875	0.862	1.109	10.3 ± 5.1
K5ac, K8ac, K12pr		0.112	0.152	0.064	
K12pr, K16ac	y_8^+	0.271	n.d.	0.012	0.2
K12ac, K16pr		0.885	1.005	1.263	
K12pr, K16ac	y_9^+	n.d.	0.123	0.054	0.02
K12ac, K16pr		2.587	4.442	6.296	

[a] Three unique spectra corresponding to the tri-acetylated and propionylated H4(4-17) tail peptide from wt H4 chromatin were analyzed. Error reported is standard deviation of the mean. n.d. = not detected.

Table 4. Comparisons of relative ion-intensities of characteristic fragment-ions from an enzymatically di-acetylated, desumoylated and chemically propionylated H4(4-17) peptide, $[M+2H]^{2+}$ = 762 Da, after activator and p300-mediated acetylation of chromatinized plasmids containing H4K12su.[a]

Species	Ion	% of Total ion intensity			Avg. ratio
K5ac, K8ac	b_5^+	2.096	2.308	1.770	71.6
K5pr, K8pr		n.d.	0.071	0.016	
K5ac, K8ac	b_6^+	2.603	2.835	2.900	33.1
K5pr, K8pr		0.053	n.d.	0.170	
K12pr, K16ac	y_6^+	0.038	0.080	n.d.	0.04
K12pr, K16pr		1.227	1.378	1.375	
K12pr, K16ac	y_8^+	0.027	0.013	0.138	0.1 ± 0.09
K12pr, K16pr		0.815	0.732	0.677	

[a] Three unique spectra corresponding to the di-acetylated and propionylated H4(4-17) tail peptide from H4K12su chromatin were analyzed. Error reported is standard deviation of the mean. n.d. = not detected.

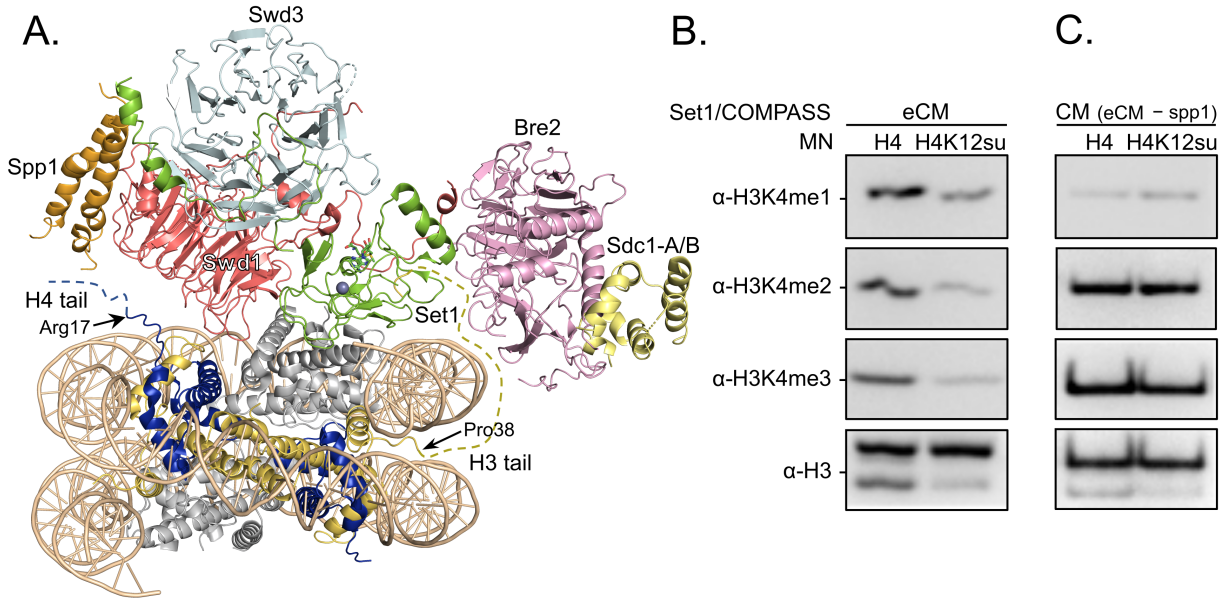

Figure 4. H3K4 methylation by the extended catalytic module of the COMPASS methyltransferase complex is inhibited by H4 sumoylation. (A) Structure of the COMPASS extended catalytic module (eCM) bound to a mononucleosome (PDB code 6UGM). The disordered H3 and H4 tails are shown in gold and blue, respectively, with the last observable amino acid indicated. Dotted lines indicate missing N-terminal amino acids. Spp1 (orange) suppressor of PRP protein 1. Swd3 (light blue), Set1 complex WD40 repeat protein 3. Swd1 (red), Set1 complex WD40 repeat protein 1. Set1 (green), SET domain protein 1. Bre2 (pink), brefeldin-A sensitivity protein 2. Sdc1-A/B (yellow), suppressor of CDC25 protein 1. (B) Western blots of the products from methylation assays with mononucleosome substrates containing wt H4 or H4K12su and the COMPASS eCM complex. Mono-, di- and trimethylated states of H3K4 were detected by the indicated modification-specific antibodies. (C) Western blots of the products from methylation assays with mononucleosome substrates containing wt H4 or H4K12su and the COMPASS catalytic module. Mono-, di- and trimethylated states of H3K4 were detected by the indicated modification-specific antibodies.

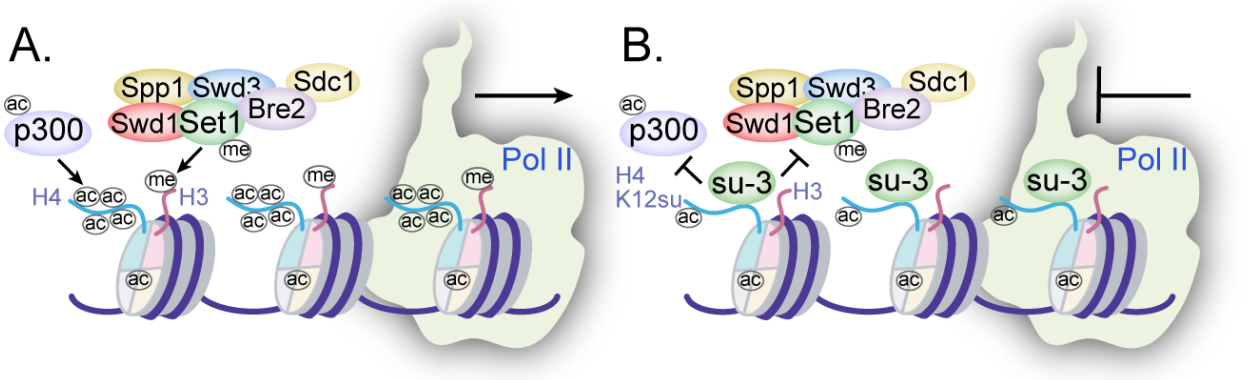

Figure 5. Mechanisms of chromatin regulation by H4K12su. (A) Transcription from chromatinized templates containing wt H4 is accompanied by acetylation of all four histones by p300, and with the methylation of the H3 tail by the COMPASS/SET1 complexes. (B) The inhibition of PolII-mediated transcription from chromatinized templates containing H4K12su is accompanied by reduced p300-mediated H4 tail acetylation. H4K12su also inhibits H3 tail methylation by the extended catalytic module of the COMPASS complex. For clarity, only one of two histone tails, each, is shown for H3 and H4.

Supplementary Figure Legends

Supplementary Figure S1. Histone octamer and mononucleosome acetylation by p300. (A) Scheme outlining the p300 histone acetyltransferase assay with octamer and mononucleosome substrates. (B) Cartoon representation of SUMO-3 showing all surface-exposed lysine residues in stick representation. The dashed line represents N-terminal residues not observed in the structure. PDB code 1U4A. (C) Coomassie-stained SDS-PAGE of purified catalytic domain of SENP2, cat.SENP2, consisting of residues 365-590. (D) Coomassie-stained SDS-PAGE of purified p300-FLAG from HEK293T cells. (E) Coomassie-stained SDS-PAGE corresponding to the HAT assay shown in Figure 1E. Asterisk indicates heat-inactivated p300 was used. (F) Histone acetylation assay with octamers containing wt H4 or H4K12su. Autoacetylation of p300 was observed with a pan-acetyllysine antibody. (G) Histone acetylation assay with p300 and wt H4 containing octamers and mononucleosomes. No cat.SENP2 was used in this assay. The asterisk indicates pre-incubation of p300-FLAG with acetyl-CoA for 1 h to allow for the build-up of activating p300-autoacetylation prior to the addition of mononucleosome substrate.[11] (H) Histone acetylation assay with wt H4 octamer with or without equimolar amounts of 147 bp Widom *601* dsDNA.

Supplementary Figure S2. Coomassie-stained SDS-PAGE of chromatin assembly proteins and in vitro transcription components. Asterisk indicates BSA used as a stabilizer.

Supplementary Figure S3. Coomassie-stained SDS-PAGE of histone acetylation assay on chromatinized plasmids containing wt H4 or H4K12su with p300 and activator Gal4-VP16. Gel bands excised for MS-MS analysis are indicated.

Supplementary Figure S4. (A) Representative MS-MS spectrum of tetra-acetylated tryptic peptide H4(4-17) generated after in vitro acetylation of chromatinized plasmids containing wt H4 with p300 and activator Gal4-VP16. (B) Peptide fragment-ion map of the tetra-acetylated H4(4-17) peptide indicating all ions identified over three spectra.

Supplementary Figure S5. (A) Representative MS-MS spectrum of tri-acetylated tryptic peptide H4(4-17) generated after in vitro acetylation of chromatinized plasmids containing wt H4 with p300 and activator Gal4-VP16. (B) Peptide fragment-ion maps of the four possible tri-acetylated H4(4-17) peptide patterns, indicating all ions identified over three spectra.

Supplementary Figure S6. (A) Representative MS-MS spectrum of di-acetylated tryptic peptide H4(4-17) generated after in vitro acetylation of chromatinized plasmids containing wt H4 with p300 and activator Gal4-VP16. (B) Peptide fragment-ion maps of the six possible di-acetylated H4(4-17) peptide patterns, indicating all ions identified over two spectra.

Supplementary Figure S7. Representative MS-MS spectrum of tri-acetylated tryptic peptide H4(4-17) generated after in vitro acetylation of chromatinized plasmids containing H4K12su with

p300 and activator Gal4-VP16 followed by in-gel desumoylation. (B) Peptide fragment-ion maps of the four possible tri-acetylated H4(4-17) peptide patterns, indicating all ions identified over three spectra. Acetylation on K12 in H4K12su is not possible due to presence of SUMO-3 at K12.

Supplementary Figure S8. Representative MS-MS spectrum of di-acetylated tryptic peptide H4(4-17) generated after in vitro acetylation of chromatinized plasmids containing H4K12su with p300 and activator Gal4-VP16 followed by desumoylation. (B) Peptide fragment-ion maps of the six possible di-acetylated H4(4-17) peptide species, indicating all ions identified over three spectra.

Supplementary Figure S9. The MS-MS spectrum of unacetylated tryptic peptide H4(4-17) after in vitro acetylation of chromatinized plasmids containing H4K12su with p300 and activator Gal4-VP16 followed by desumoylation. (B) Peptide fragment-ion map of the unmodified H4(4-17) peptide, indicating identified ions.

Supplementary Figure S10. Coomassie-stained SDS-PAGE gel of recombinant *K. lactis* COMPASS CM and COMPASS eCM sub-complexes used in H3K4 methylation assays. The Sdc1 subunit (10 kDa) is not observed on this gel due to its size. Set1-SET is the catalytic domain. Set1-N674 includes the nSET domain, beginning at residue 674.

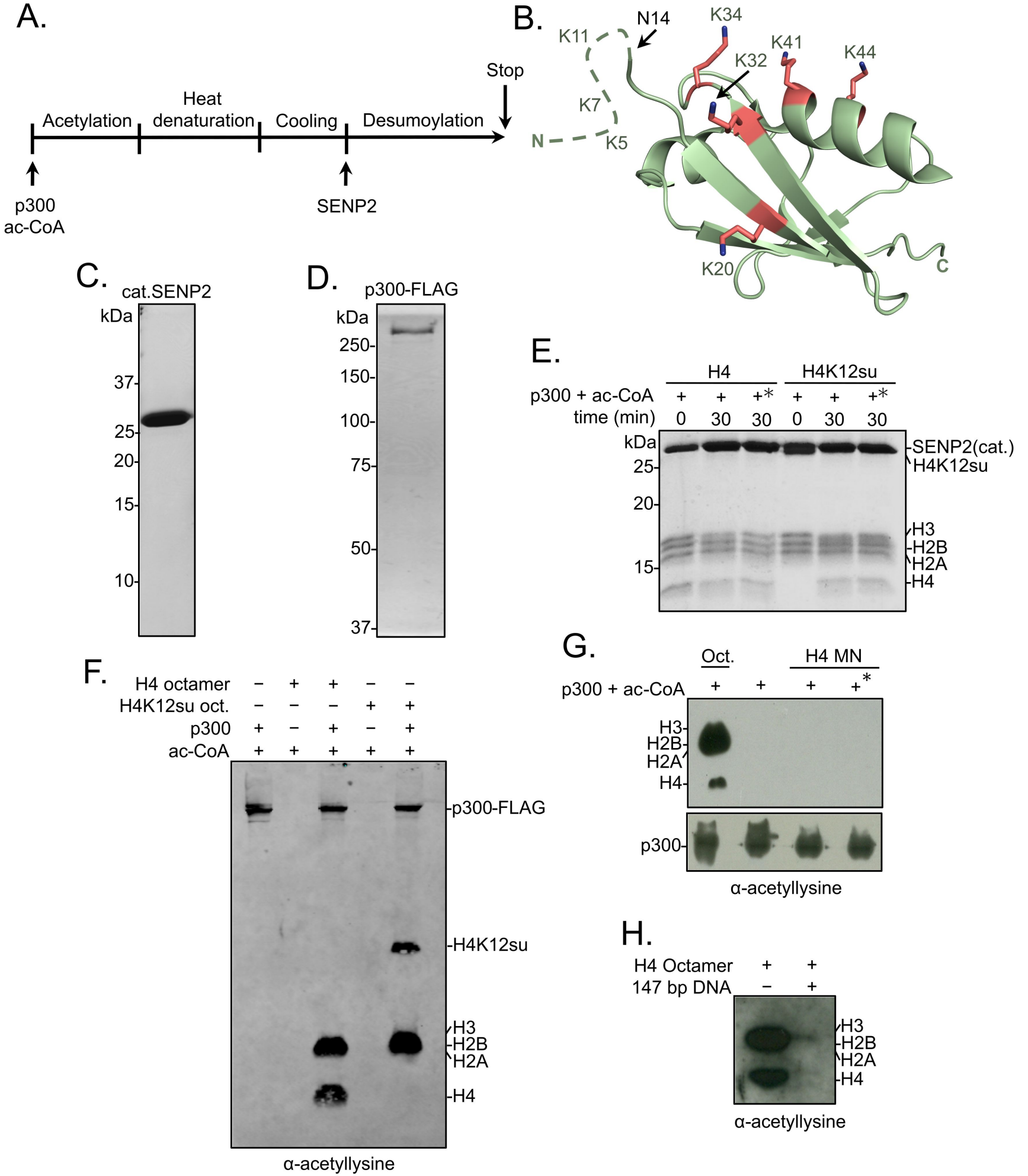
A.
Acetylation
Heat denaturation
Cooling
Desumoylation
Stop
p300 ac-CoA
SENP2
B.
N14
K34
K11
K41
K32
K44
K7
N
K5
K20
C
C.
cat.SENP2
kDa
37
25
20
15
10
D.
p300-FLAG
kDa
250
150
100
75
50
37
E.
H4
H4K12su
p300 + ac-CoA
+ + +* + + +*
time (min)
0 30 30 0 30 30
kDa
25
20
15
SENP2(cat.)
H4K12su
H3
H2B
H2A
H4
F.
H4 octamer
H4K12su oct.
p300
ac-CoA
p300-FLAG
H4K12su
H3
H2B
H2A
H4
α-acetyllysine
G.
Oct.
H4 MN
p300 + ac-CoA
H3
H2B
H2A
H4
p300
α-acetyllysine
H.
H4 Octamer
147 bp DNA
H3
H2B
H2A
H4
α-acetyllysine

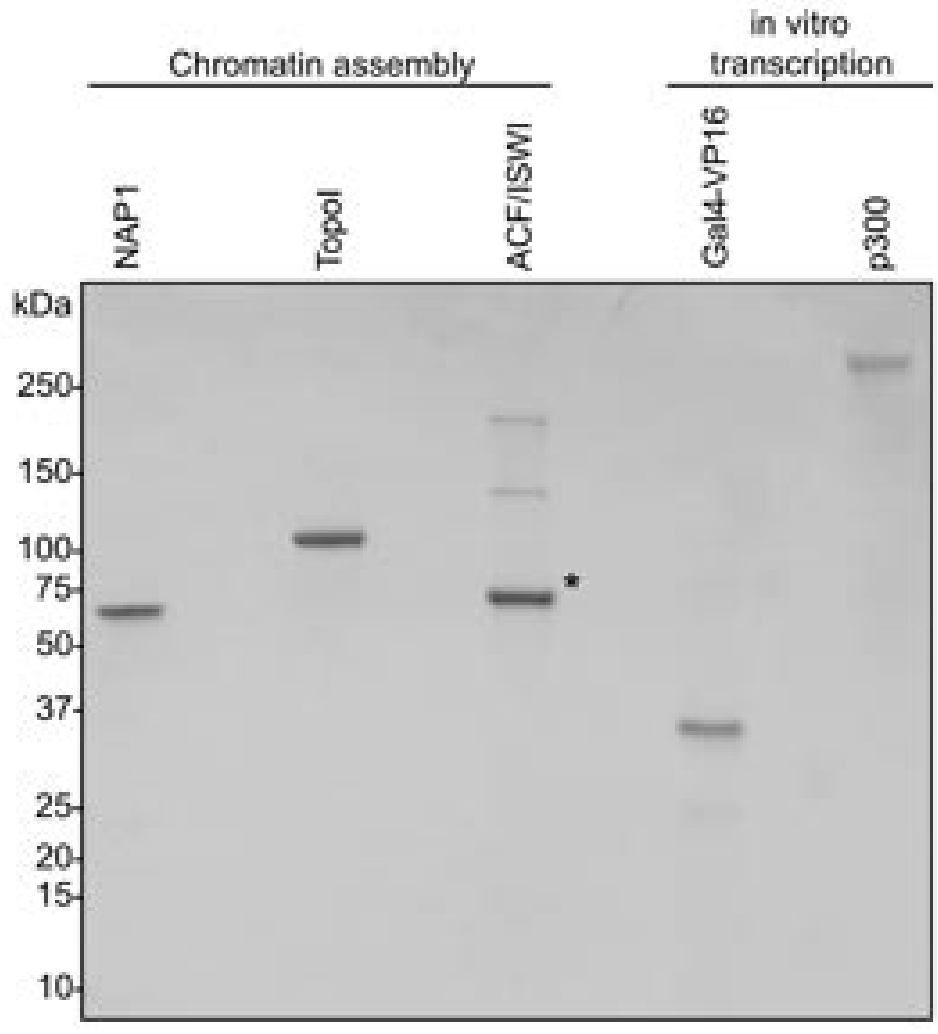
Chromatin assembly
in vitro transcription
NAP1
Topoi
ACF/ISWI
Gal4-VP16
p300
kDa
250
150
100
75
50
37
25
20
15
10
*

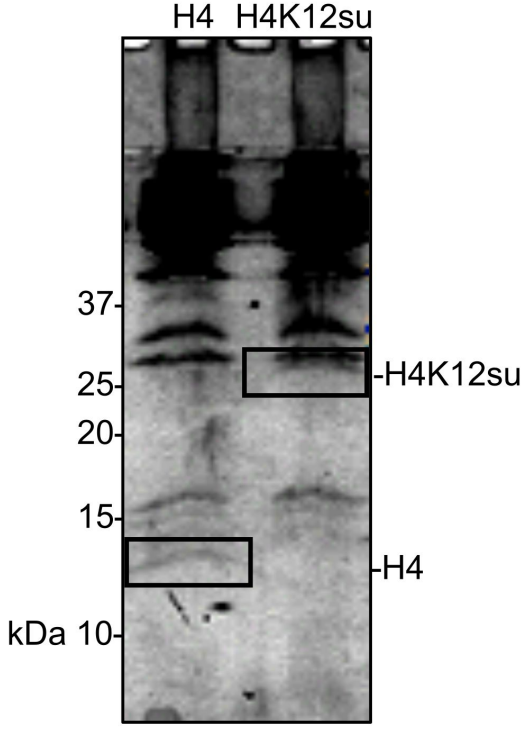
H4
H4K12su
37
25
20
15
kDa 10
H4K12su
H4

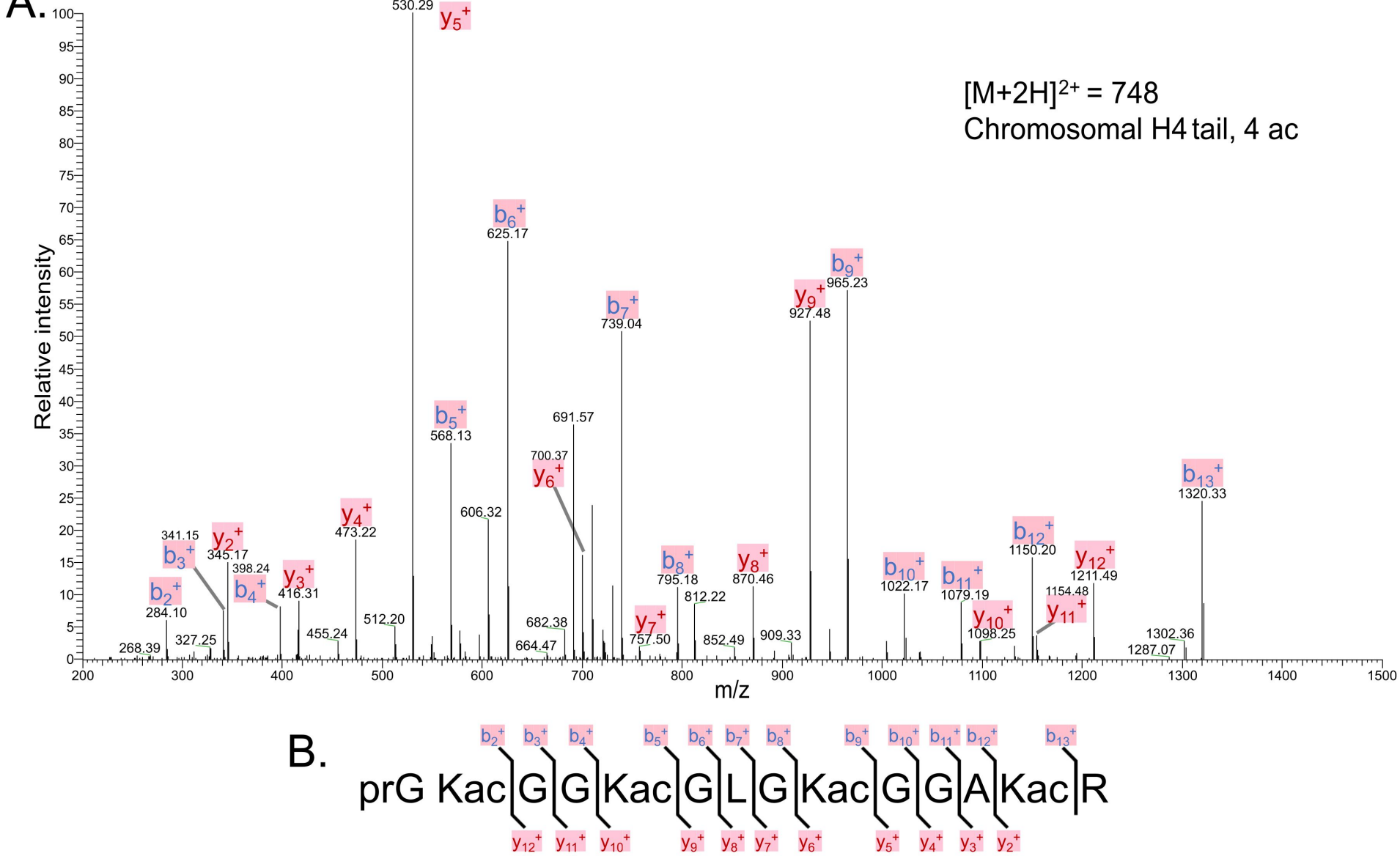
A.
[M+2H]2+ = 748
Chromosomal H4 tail, 4 ac
Relative intensity
m/z
530.29 y5+
b6+ 625.17
b7+ 739.04
b9+ 965.23
y9+ 927.48
b5+ 568.13
691.57
700.37 y6+
606.32
y4+ 473.22
341.15 b3+
y2+ 345.17
398.24 b4+
y3+ 416.31
b2+ 284.10
268.39
327.25
455.24
512.20
682.38
664.47
y7+ 757.50
b8+ 795.18
812.22
y8+ 870.46
852.49
909.33
b10+ 1022.17
b11+ 1079.19
b12+ 1150.20
y12+ 1211.49
1154.48 y11+
y10+ 1098.25
b13+ 1320.33
1302.36
1287.07
B.
prG Kac G G Kac G L G Kac G G A Kac R
b2+ b3+ b4+ b5+ b6+ b7+ b8+ b9+ b10+ b11+ b12+ b13+
y12+ y11+ y10+ y9+ y8+ y7+ y6+ y5+ y4+ y3+ y2+

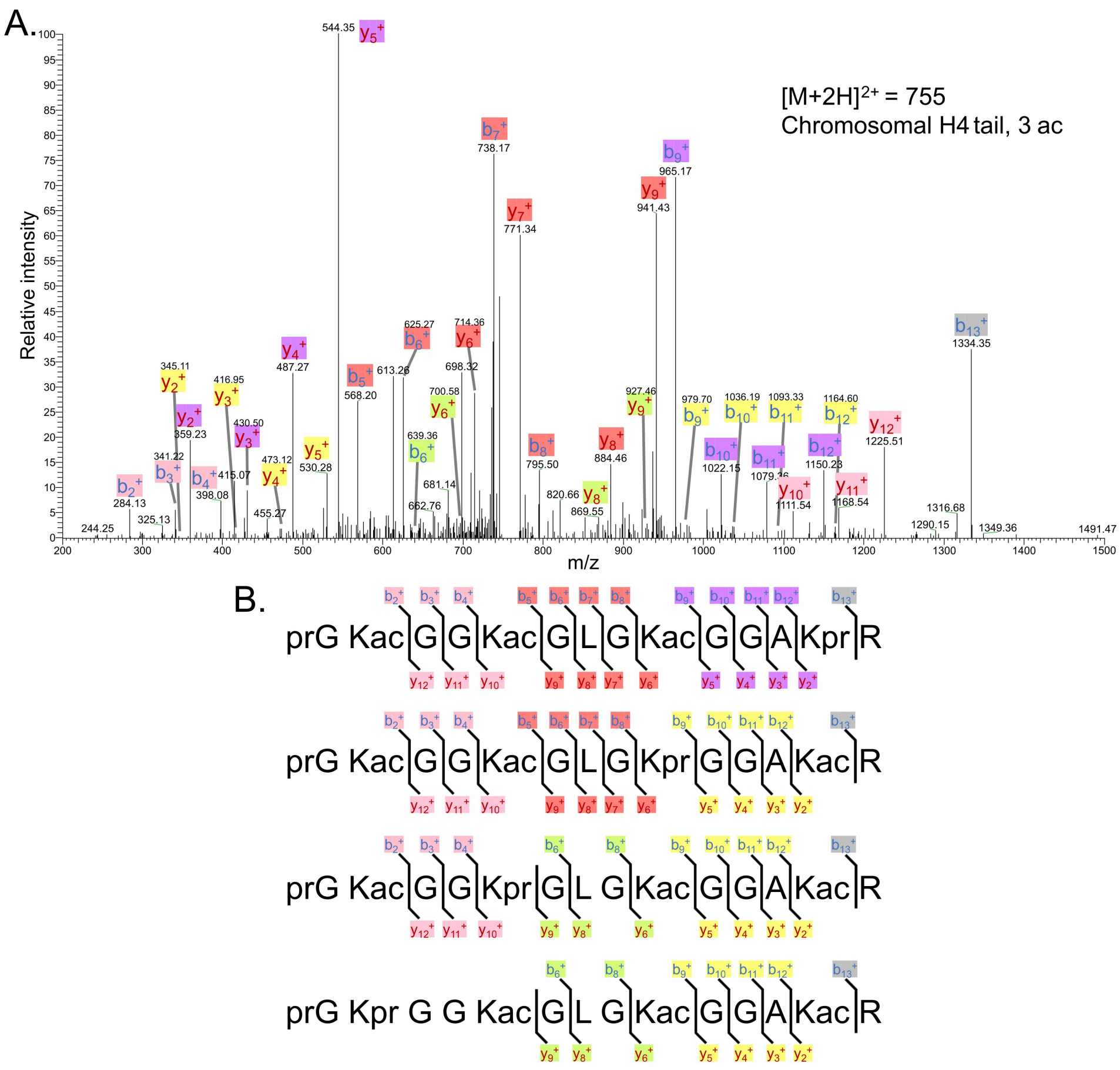
A.
[M+2H]2+ = 755
Chromosomal H4 tail, 3 ac
Relative intensity
m/z
B.
prG Kac G G Kac G L G Kac G G A Kpr R
prG Kac G G Kac G L G Kpr G G A Kac R
prG Kac G G Kpr G L G Kac G G A Kac R
prG Kpr G G Kac G L G Kac G G A Kac R

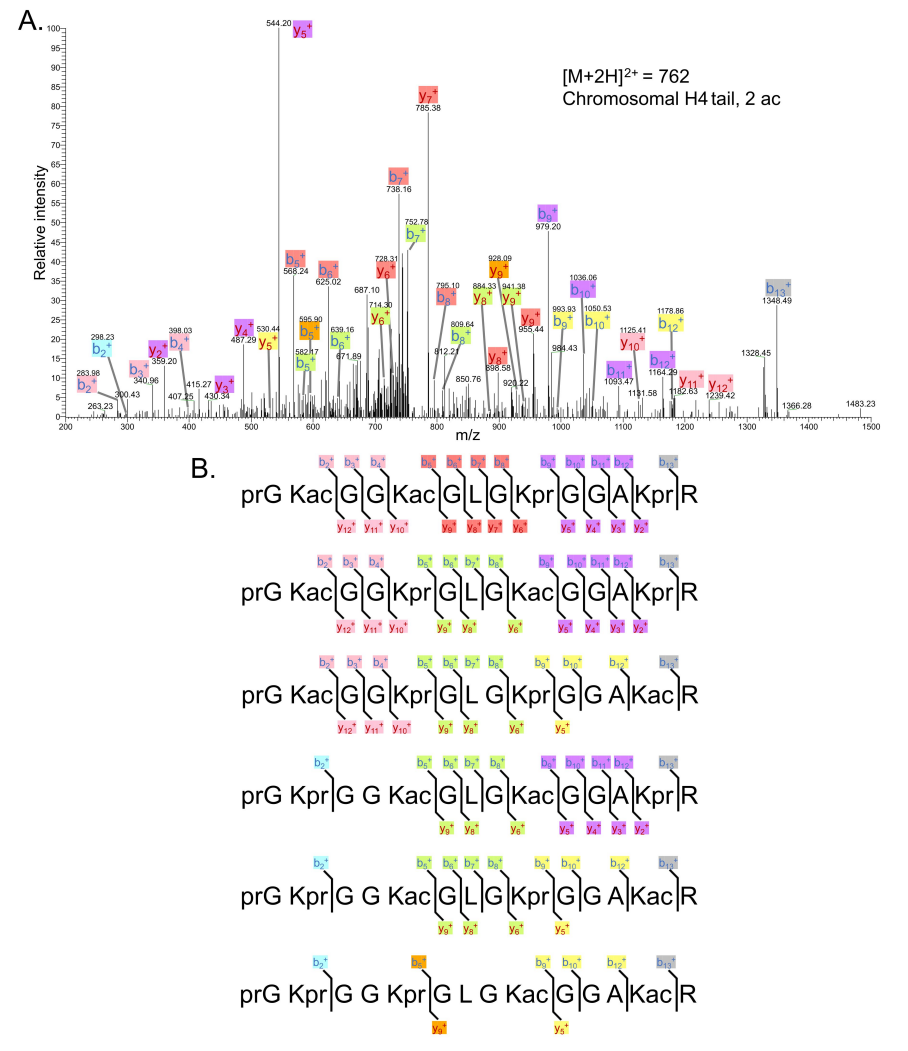
A.
[M+2H]2+ = 762
Chromosomal H4 tail, 2 ac
Relative intensity
m/z
B.
prG Kac G G Kac G L G Kpr G G A Kpr R
prG Kac G G Kpr G L G Kac G G A Kpr R
prG Kac G G Kpr G L G Kpr G G A Kac R
prG Kpr G G Kac G L G Kac G G A Kpr R
prG Kpr G G Kac G L G Kpr G G A Kac R
prG Kpr G G Kpr G L G Kac G G A Kac R

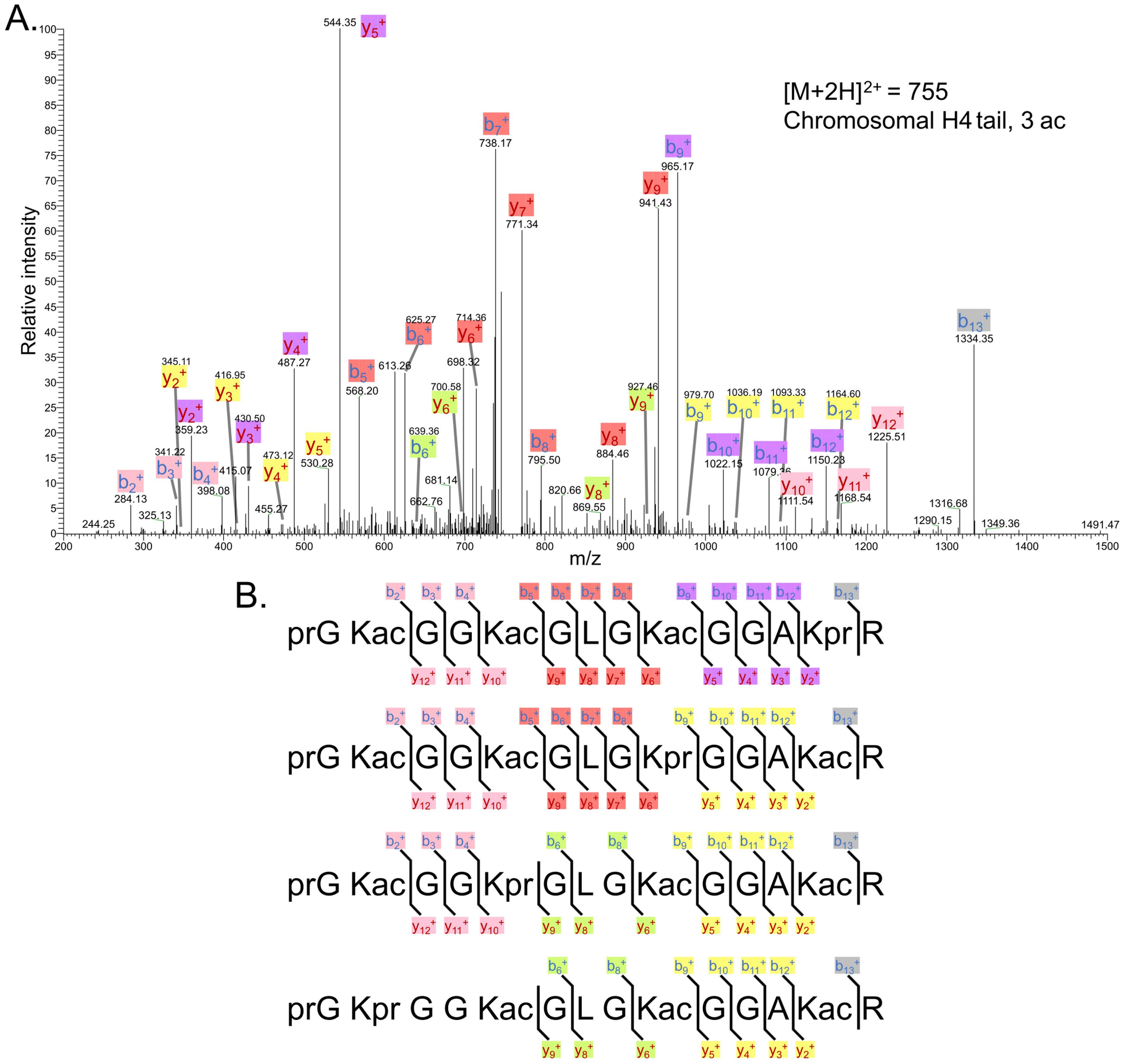
A.
[M+2H]2+ = 755
Chromosomal H4 tail, 3 ac
Relative intensity
m/z
544.35 y5+
738.17 b7+
965.17 b9+
941.43 y9+
771.34 y7+
625.27 b6+
714.36 y6+
487.27 y4+
345.11 y2+
613.26
698.32
568.20 b5+
416.95 y3+
700.58 y6+
927.46 y9+
979.70 b9+
1036.19 b10+
1093.33 b11+
1164.60 b12+
1334.35 b13+
359.23 y2+
430.50 y3+
639.36 b6+
795.50 b8+
884.46 y8+
1225.51 y12+
341.22 b3+
530.28 y5+
473.12 y4+
1022.15 b10+
1150.23 b12+
284.13 b2+
415.07 b4+
398.08
681.14
1079.16 b11+
1111.54 y10+
1168.54 y11+
820.66
869.55 y8+
662.76
455.27
325.13
244.25
1316.68
1290.15
1349.36
1491.47
B.
prG Kac G G Kac G L G Kac G G A Kpr R
prG Kac G G Kac G L G Kpr G G A Kac R
prG Kac G G Kpr G L G Kac G G A Kac R
prG Kpr G G Kac G L G Kac G G A Kac R

A.

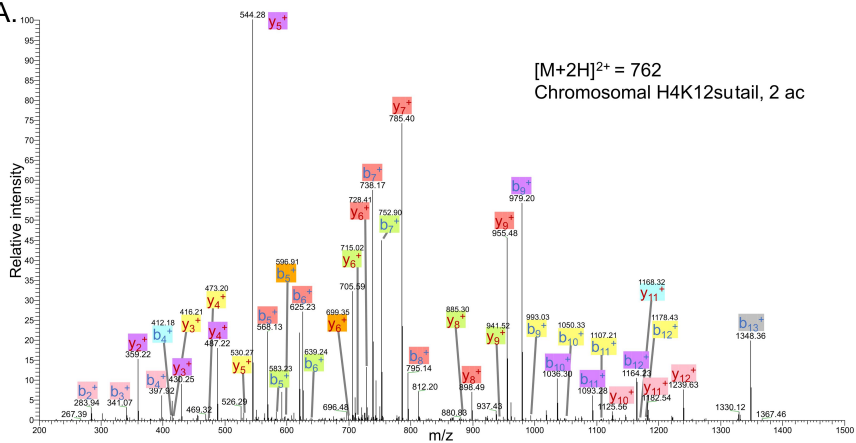
[M+2H]2+ = 762
Chromosomal H4K12sutail, 2 ac
Relative intensity
m/z

B.

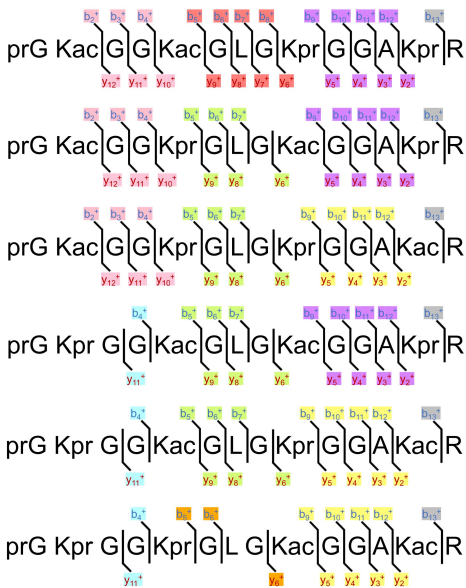
prG Kac G G Kac G L G Kpr G G A Kpr R
prG Kac G G Kpr G L G Kac G G A Kpr R
prG Kac G G Kpr G L G Kpr G G A Kac R
prG Kpr G G Kac G L G Kac G G A Kpr R
prG Kpr G G Kac G L G Kpr G G A Kac R
prG Kpr G G Kpr G L G Kac G G A Kac R

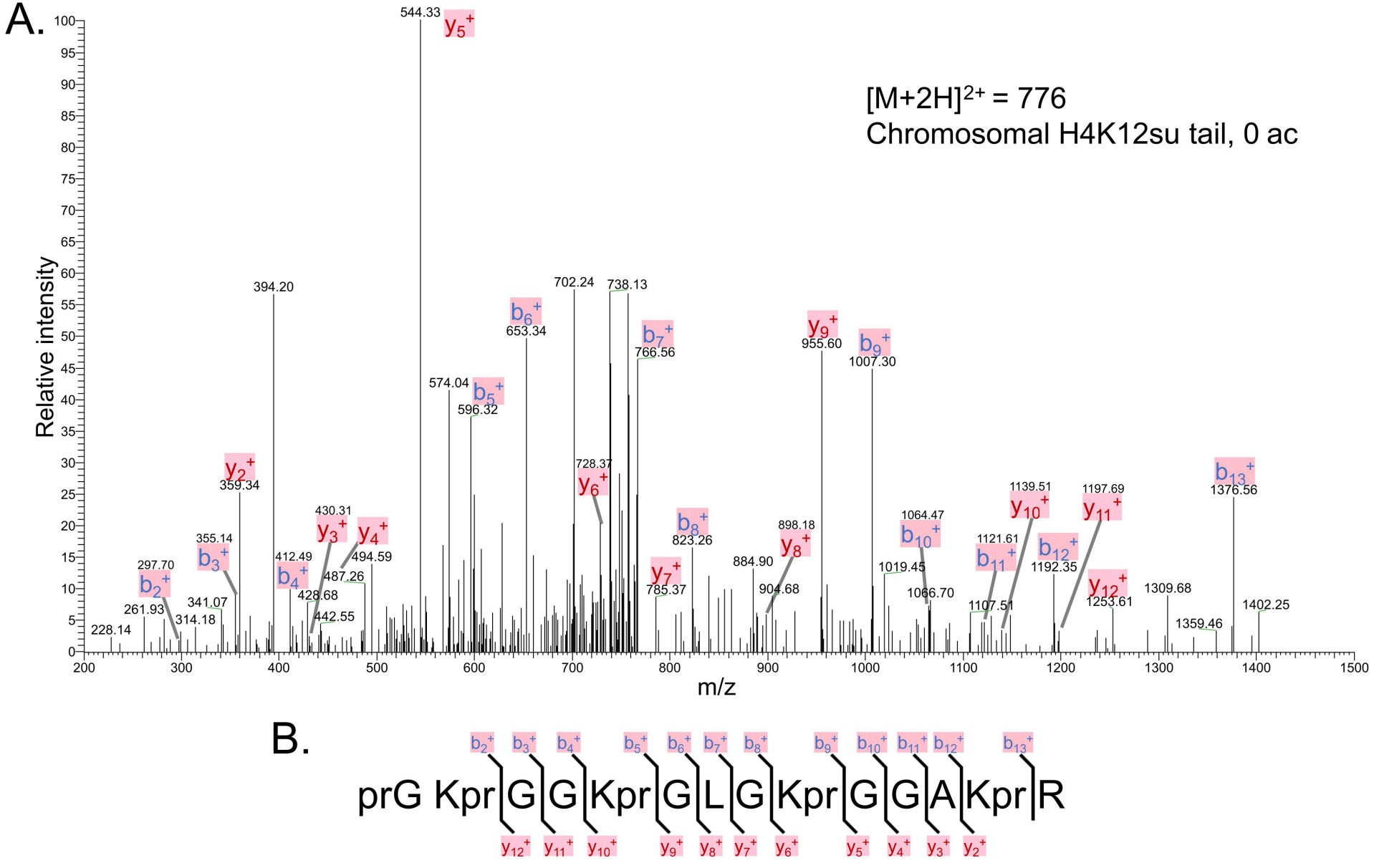
A.
[M+2H]2+ = 776
Chromosomal H4K12su tail, 0 ac
Relative intensity
m/z
544.33 y5+
394.20
702.24
738.13
b6+ 653.34
b7+ 766.56
y9+ 955.60
b9+ 1007.30
574.04
b5+ 596.32
728.37 y6+
y2+ 359.34
430.31 y3+
y4+
b8+ 823.26
898.18 y8+
1139.51 y10+
1197.69 y11+
b13+ 1376.56
1064.47 b10+
b12+ 1192.35
1121.61 b11+
355.14 b3+
412.49 b4+
297.70 b2+
487.26
494.59
884.90
y7+ 785.37
904.68
1019.45
1066.70
1107.51
y12+ 1253.61
1309.68
1402.25
1359.46
261.93
341.07
314.18
428.68
442.55
228.14
B.
b2+ b3+ b4+ b5+ b6+ b7+ b8+ b9+ b10+ b11+ b12+ b13+
prG Kpr G G Kpr G L G Kpr G G A Kpr R
y12+ y11+ y10+ y9+ y8+ y7+ y6+ y5+ y4+ y3+ y2+

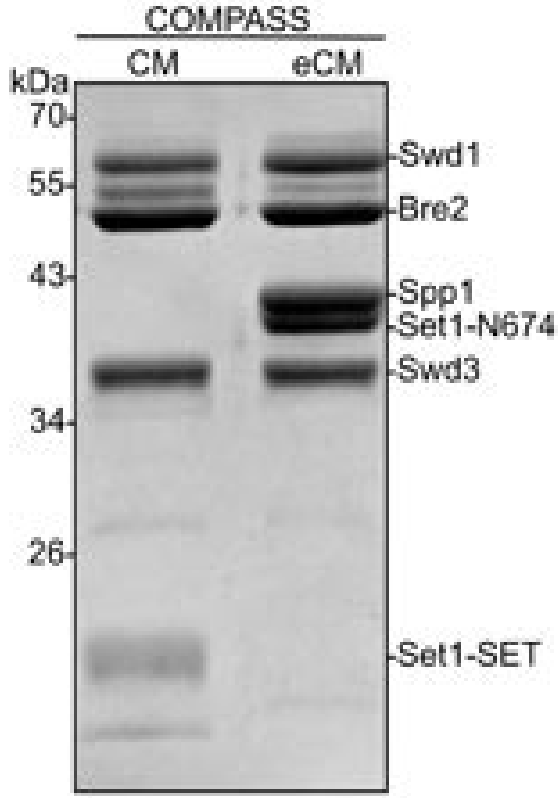
COMPASS
CM
eCM
kDa
70
55
43
34
26
Swd1
Bre2
Spp1
Set1-N674
Swd3
Set1-SET